

# SHA-1 is a Shambles\*

## First Chosen-Prefix Collision on SHA-1 and Application to the PGP Web of Trust

Gaëtan Leurent<sup>1</sup> and Thomas Peyrin<sup>2,3</sup>

<sup>1</sup> Inria, France

<sup>2</sup> Nanyang Technological University, Singapore

<sup>3</sup> Temasek Laboratories, Singapore

[gaetan.leurent@inria.fr](mailto:gaetan.leurent@inria.fr), [thomas.peyrin@ntu.edu.sg](mailto:thomas.peyrin@ntu.edu.sg)

<https://sha-mbles.github.io/>

**Abstract.** The *SHA-1* hash function was designed in 1995 and has been widely used during two decades. A theoretical collision attack was first proposed in 2004 [29], but due to its high complexity it was only implemented in practice in 2017, using a large GPU cluster [23]. More recently, an almost practical *chosen-prefix* collision attack against *SHA-1* has been proposed [12]. This more powerful attack allows to build colliding messages with two arbitrary prefixes, which is much more threatening for real protocols.

In this paper, we report the first practical implementation of this attack, and its impact on real-world security with a PGP/GnuPG impersonation attack. We managed to significantly reduce the complexity of collision attacks against *SHA-1*: on an Nvidia GTX 970, identical-prefix collisions can now be computed with a complexity (expressed in terms of *SHA-1* equivalents on this GPU) of  $2^{61.2}$  rather than  $2^{64.7}$ , and chosen-prefix collisions with a complexity of  $2^{63.4}$  rather than  $2^{67.1}$ . When renting cheap GPUs, this translates to a cost of US\$ 11k for a collision, and US\$ 45k for a chosen-prefix collision, within the means of academic researchers. Our actual attack required two months of computations using 900 Nvidia GTX 1060 GPUs (we paid US\$ 75k because GPU prices were higher, and we wasted some time preparing the attack).

Therefore, the same attacks that have been practical on *MD5* since 2009 are now practical on *SHA-1*. In particular, chosen-prefix collisions can break signature schemes and handshake security in secure channel protocols (TLS, SSH), if generated extremely quickly. We strongly advise to remove *SHA-1* from those type of applications as soon as possible.

We exemplify our cryptanalysis by creating a pair of PGP/GnuPG keys with different identities, but colliding *SHA-1* certificates. A *SHA-1* certification of the first key can therefore be transferred to the second key, leading to an impersonation attack. This proves that *SHA-1* signatures now offer virtually no security in practice. The legacy branch of GnuPG still uses *SHA-1* by default for identity certifications, but after notifying the authors, the modern branch now rejects *SHA-1* signatures (the issue is tracked as CVE-2019-14855).

**Keywords:** *SHA-1* · Cryptanalysis · Chosen-prefix collision · HPC · GPU · PGP · GnuPG

---

\*This is the full version of the paper of the same title published at USENIX Security '20.

## 1 Introduction

Cryptographic hash functions are present in countless security applications and protocols, used for various purposes such as building digital signature schemes, message authentication codes or password hashing functions. In the key application of digital signatures for example, hash functions are classically applied on the message before signing it, as a domain extender and also to provide security guarantees. Informally, a cryptographic hash function  $H$  is a function that maps an arbitrarily long message  $M$  to a fixed-length hash value (we denote  $n$  its bit size). *Collision resistance* is the main security property expected from a hash function: it should be hard for an adversary to compute a collision (or *identical-prefix* collision), i.e. two distinct messages  $M$  and  $M'$  that map to the same hash value  $H(M) = H(M')$ , where by “hard” one means not faster than the generic  $2^{n/2}$  computations birthday attack.

A cryptanalyst will try to find a collision for the hash function at a reduced cost, but ad-hoc collision attacks are hard to exploit in practice, because the attacker usually has little control over the value of the actual colliding messages (in particular where the differences are inserted, which are the interesting parts when attacking a digital signature scheme). Thus, one can consider stronger variants of the collision attack more relevant in practice, such as the so-called *chosen-prefix* collision [25] or CP collision. Two message prefixes  $P$  and  $P'$  are first given as challenge to the adversary, and his goal is to compute two messages  $M$  and  $M'$  such that  $H(P \parallel M) = H(P' \parallel M')$ , where  $\parallel$  denotes concatenation. With such ability, the attacker can obtain a collision with arbitrarily chosen prefixes, potentially containing meaningful information. A CP collision can also be found generically with  $2^{n/2}$  computations (thus  $2^{80}$  for a 160-bit hash function like **SHA-1**), but ad-hoc CP collision attacks are much more difficult to find than plain collision attacks, because of the uncontrolled internal differences created by the prefixes. Yet, a CP collision attack was found for the **MD5** hash function [25], eventually leading to the creation of colliding X.509 certificates, and later of a rogue Certificate Authority (CA) [27]. CP collisions have also been shown to break important internet protocols, including TLS, IKE, and SSH [1], because they allow forgeries of the handshake messages if they can be generated extremely quickly.

Largely inspired by **MD4** [19] and then **MD5** [20], **SHA-1** [16] is one the most famous cryptographic hash functions in the world, having been the NIST and de-facto worldwide hash function standard for nearly two decades. It remained a NIST standard until its deprecation in 2011 (and was forbidden for digital signatures at the end of 2013). Indeed, even though its successors **SHA-2** or **SHA-3** are believed to be secure, **SHA-1** has been broken by a theoretical collision attack in 2004 [29]. Due to its high technicality and computational complexity (originally estimated to about  $2^{69}$  hash function calls), this attack was only implemented in practice in 2017, using a large GPU cluster [23]. Unfortunately, the **SHA-1** deprecation process has been quite slow and one can still observe many uses of **SHA-1** in the wild, because it took more than a decade to compute an actual collision, plain collisions are difficult to use directly to attack a protocol, and migration is expensive. Web browsers have recently started to reject certificates with **SHA-1** signatures, but there are still many users with older browsers, and many protocols and software that allow **SHA-1** signatures. As observed in [12], it is still possible to buy a **SHA-1** certificate from a trusted CA, many email clients accept a **SHA-1** certificate when opening a TLS connection, and **SHA-1** is also widely supported to authenticate TLS handshake messages.

Very recently, a CP collision attack against **SHA-1** has been described in [12] (but not implemented), which requires an estimated complexity between  $2^{66.9}$  and  $2^{69.4}$  **SHA-1** computations. It works with a two-phase strategy: given the challenge prefixes and the random differences on the internal state it will induce, the first part of the attack uses a birthday approach to limit the internal state differences to a not-too-big subset (as done in [25, 22]). From this subset, reusing basic principles of the various collision search

**Table 1:** Comparison of previous and new cryptanalysis results on **SHA-1**. A free-start collision is a collision of the compression function only, where the attacker has full control on all the primitive’s inputs. Complexities in the table are given in terms of **SHA-1** equivalents on a GTX-970 GPU (when possible).

Function	Collision type	Complexity	Ref.
SHA-1	free-start collision	$2^{57.5}$	[24]
		$2^{69}$	[29]
		$2^{64.7}$	[22, 23] <sup>a</sup>
	chosen-prefix collision	$2^{61.2}$	New
		$2^{77.1}$	[22]
		$2^{67.1}$	[12]
		$2^{63.4}$	New

<sup>a</sup>Equivalent to  $2^{61}$  **SHA-1** on CPU,  $2^{64.7}$  on GPU

advances on **SHA-1**, one slowly adds successive message blocks to come closer to a collision, eventually reaching the goal after a dozen blocks. Even though these advances put the CP collisions within practical reach for very well-funded entities, it remains very expensive to conduct and also very difficult to implement as the attack contains many very technical parts.

## 1.1 Our Contributions

In this article, we exhibit the very first chosen-prefix collision against **SHA-1**, with a direct application to PGP/GnuPG security. Our contributions are threefold.

**Complexity improvements.** While the work of [12] was mostly about high-level techniques to turn a collision attack into a chosen-prefix collision attack, we have to look at the low-level details to actually implement the attack. This gave us a better understanding of the complexity of the attack, and we managed to significantly improve several parts of the attacks (See Table 1).

First, we have improved the use of degrees of freedom (neutral bits [3] and boomerangs [10]) during the search for near-collision blocks. This reduces the computational complexity for both plain and chosen-prefix collision attacks, leading to important savings: on an Nvidia GTX 970, plain collisions can now be computed with a complexity of  $2^{61.2}$  rather than  $2^{64.7}$  (expressed in terms of **SHA-1** equivalents on this GPU). We note that the general ideas underlying these improvements might be interesting for cryptanalysis of algorithms beyond **SHA-1**.

Second, we improved the graph-based technique of [12] to compute a chosen-prefix collision. Using a larger graph and more heuristic techniques, we can significantly reduce the complexity of a chosen-prefix collision attack, taking full advantage of the improvements on the near-collision block search. This results in a chosen-prefix collision attack with a complexity of  $2^{63.4}$  rather than  $2^{67.1}$ .

**Record computation.** We have implemented the entire chosen-prefix collision attack from [12], with those improvements. This attack is extremely technical, contains many details, various steps, and requires a lot of engineering work. Performing such a large-scale computation is still quite expensive, but is accessible with an academic budget. More precisely, we can rent cheap GPUs from providers that use gaming or mining cards in consumer-grade PCs, rather than the datacenter-grade hardware used by big

**Table 2:** Complexity of the attacks against SHA-1 reported in this paper on several GPUs. The complexity is given in SHA-1 equivalents (using hashcat benchmarks). For the cost evaluation we assume that one GTX 1060 GPU can be rented for a price of US\$ 35/month (the two phases of the attack are easily parallelisable): <https://web.archive.org/web/20191229164814/https://www.gpuserversrental.com/>

To attack MD5 || SHA-1, we use the multicollision attack of Joux [9] with three phases: (i) a CP collision on SHA-1, (ii) 64 collisions on SHA-1, and (iii)  $2^{64}$  evaluations of MD5.

Function	Collision type	GPU	Time	Complexity	Cost
SHA-1	collision	GTX 970	22 years	$2^{61.2}$	US\$ 11k
		GTX 1060	27 years	$2^{61.6}$	
		GTX 1080 Ti	8 years	$2^{61.6}$	
	chosen-prefix	GTX 970	99 years	$2^{63.4}$	US\$ 45k
		GTX 1060	107 years	$2^{63.5}$	
		GTX 1080 Ti	34 years	$2^{63.6}$	
MD5    SHA-1	both (plain or CP)	GTX 970	1400 years	$2^{67.2}$	US\$ 720k
		GTX 1060	1700 years	$2^{67.6}$	
		GTX 1080 Ti	540 years	$2^{67.6}$	

cloud providers. This gives a total cost significantly smaller than US\$ 100k to compute a chosen-prefix collision. We give more detailed complexity and cost estimates in Table 2.

We have successfully run the computation over a period of two months, using 900 GPUs (Nvidia GTX 1060). Our attack uses one partial block for the birthday stage, and 9 near-collision blocks. We paid US\$ 75k to rent the GPUs from GPUUsersrental, but the actual price could be smaller because we lost some time tuning the attack. There is also a large variability depending on luck, and GPU rental prices fluctuate with cryptocurrency prices.

**PGP/GnuPG impersonation.** Finally, in order to demonstrate the practical impact of chosen-prefix collisions, we used our CP collision for a PGP/GnuPG impersonation attack. The chosen prefixes correspond to headers of two PGP identity certificates with keys of different sizes, an RSA-8192 key and an RSA-6144 key. By exploiting properties of the OpenPGP and JPEG format, we can create two public keys (and their corresponding private keys): key A with the victim name, and key B with the attacker name and picture, such that the identity certificate containing the attacker key and picture leads to the same SHA-1 hash as the identity certificate containing the victim key and name. Therefore, the attacker can request a signature of his key and picture from a third party (from the Web of Trust or from a CA) and transfer the signature to key A. The signature stays valid because of the collision, while the attacker controls key A with the name of the victim, and signed by the third party. Therefore, he can impersonate the victim and sign any document in her name.

## 1.2 SHA-1 Usage and Impact

Our work shows that SHA-1 is now fully and practically broken for use in digital signatures. GPU technology improvements and general computation cost decrease will further reduce the cost, making it affordable for any ill-intentioned attacker in the very near future.

SHA-1 usage has significantly decreased in the last years; in particular web browsers now reject certificates signed with SHA-1. However, SHA-1 signatures are still supported in a large number of applications. SHA-1 is the default hash function used for certifying PGP keys in the legacy branch of GnuPG (v 1.4), and those signatures were accepted by

the modern branch of GnuPG (v 2.2) before we reported our results. Many non-web TLS clients also accept **SHA-1** certificates, and **SHA-1** is still allowed for in-protocol signatures in TLS and SSH. Even if actual usage is low (a few percent), the fact that **SHA-1** is *allowed* threatens the security because a man-in-the-middle attacker can downgrade the connection to **SHA-1**. **SHA-1** is also the foundation of the GIT versioning system, and it is still in DNSSEC signatures. There are probably a lot of less known or proprietary protocols that still use **SHA-1**, but this is more difficult to evaluate.

### 1.3 Outline

We first recall **SHA-1** inner workings and previous cryptanalysis on this hash function in Section 2. We then provide improvements over the state-of-the-art **SHA-1** collision attacks in Section 3 and Section 4, and we describe the details of the **SHA-1** chosen-prefix collision computation in Section 5. Finally, we show a direct application of our CP collision attack with a PGP/GnuPG impersonation (together with discussions on other possible applications) in Section 6. We discuss **SHA-1** usage and the impact of our results in Section 7. Eventually, we conclude and propose future works in Section 8.

## 2 Preliminaries

In this section, we describe the **SHA-1** hash function (we refer to [16] for all the complete details) and summarize the previous cryptanalysis relevant to our new work.

### 2.1 Description of **SHA-1**

**SHA-1** is a 160-bit hash function that follows the well-known Merkle-Damgård [6, 15] paradigm. A padding is first applied to the message input (with message length encoded) so that we obtain a multiple of 512 bits, and this bit string is divided into blocks  $m_i$  of 512 bits each. Then, each block  $m_i$  is processed via the **SHA-1** compression function (denoted  $h$ ) to update a 160-bit chaining variable (denoted  $cv_i$ ) that is initialised to a constant and public initial value (denoted  $IV$ ):  $cv_0 = IV$ . More precisely, we have  $cv_{i+1} = h(cv_i, m_{i+1})$ . When all blocks have eventually been processed, the last chaining variable is the final hash output.

The **SHA-1** compression function resembles other members of the MD-SHA family of hash functions. It uses the Davies-Meyer construction, that turns a block cipher  $E$  into a compression function:  $cv_{i+1} = E_{m_{i+1}}(cv_i) + cv_i$ , where  $E_k(y)$  is the encryption of the plaintext  $y$  with the key  $k$ , and  $+$  is a word-wise modular addition.

The internal block cipher is composed of 4 rounds of 20 steps each (for a total of 80 steps), where one step follows a generalised Feistel network. More precisely, the internal state is divided into five registers  $(A_i, B_i, C_i, D_i, E_i)$  of 32-bit each and at each step, an extended message word  $W_i$  updates the registers as follows:

$$\begin{cases} A_{i+1} &= (A_i \lll 5) + f_i(B_i, C_i, D_i) + E_i + K_i + W_i \\ B_{i+1} &= A_i \\ C_{i+1} &= B_i \ggg 2 \\ D_{i+1} &= C_i \\ E_{i+1} &= D_i \end{cases}$$

where  $K_i$  are predetermined constants and  $f_i$  are boolean functions (in short: IF function for the first round, XOR for the second and fourth round, MAJ for the third round, see Table 3). Since only a single register value is updated, we can express the **SHA-1** step function using a single variable:

$$A_{i+1} = (A_i \lll 5) + f_i(A_{i-1}, A_{i-2} \ggg 2, A_{i-3} \ggg 2) + (A_{i-4} \ggg 2) + K_i + W_i.$$

**Table 3:** Boolean functions and constants of SHA-1

step $i$	$f_i(B, C, D)$	$K_i$
$0 \leq i < 20$	$f_{IF} = (B \wedge C) \oplus (\overline{B} \wedge D)$	0x5a827999
$20 \leq i < 40$	$XOR = B \oplus C \oplus D$	0x6ed6eba1
$40 \leq i < 60$	$MAJ = (B \wedge C) \oplus (B \wedge D) \oplus (C \wedge D)$	0x8fabbcdc
$60 \leq i < 80$	$XOR = B \oplus C \oplus D$	0xca62c1d6

For this reason, the differential trails figures in this article will only represent  $A_i$ , the other register values at a certain point of time can be deduced directly.

The extended message words  $W_i$  are computed linearly from the incoming 512-bit message block  $m$ , the process being called message extension. One first splits  $m$  into 16 32-bit words  $M_0, \dots, M_{15}$ , and then the  $W_i$ 's are computed as follows:

$$W_i = \begin{cases} M_i, & \text{for } 0 \leq i \leq 15 \\ (W_{i-3} \oplus W_{i-8} \oplus W_{i-14} \oplus W_{i-16}) \lll 1, & \text{for } 16 \leq i \leq 79 \end{cases}$$

In the rest of this article, we will use the notation  $X[j]$  to refer to bit  $j$  of word  $X$ .

## 2.2 Previous Works

We recall here the general state-of-the-art collision search strategies that we will use for our CP collision attack. Readers only interested by the applications of our CP collision attack can skip up to Section 6. In the rest of the article, unless stated otherwise, difference will refer to the XOR difference between two bits or the bitwise XOR difference between two words.

### 2.2.1 Differential Trails

The first results on SHA-0 (the predecessor of SHA-1) and SHA-1 were differential in nature and obtained by building differential paths from a linearization of the compression function (we call these *linear paths*, in opposition to *non-linear paths* which have been built without linearization): in order to simplify the analysis the attacker assumes that modular additions and boolean functions  $f_i$  in the SHA-1 compression function are behaving as an XOR with regards to differential propagation. More precisely, the 32-bit modular addition is replaced by a 32-bit bitwise XOR and the  $f_i$  functions are replaced by 3-input XOR operations. These assumptions are indeed happening with a certain probability, which will basically consist of the bulk of the final attack cost. Then, in order to further simplify the analysis while trying to minimize the number of differences present in the internal state (which will in turn increase the differential trail probability and therefore improve the final attack cost), these trails are generated with a succession of so-called local collisions: small message disturbances whose influence is immediately corrected with other message differences inserted in the subsequent SHA-1 steps, while following the SHA-1 message expansion. However, in this linearization model, impossibilities might appear in the first 20 steps of SHA-1 (as in some specific cases the  $f_{IF}$  boolean function will never behave as a 3-input XOR with regards to differential propagation) and the cheapest trail candidates might not be the ones that start and end with the same difference (which is a property required to obtain directly a 1-block collision after the compression function feed-forward). This strategy could already break the collision resistance of SHA-0, but not yet for SHA-1 (due to a small rotation added in the message expansion of SHA-1, that forces disturbances to spread throughout the rounds).

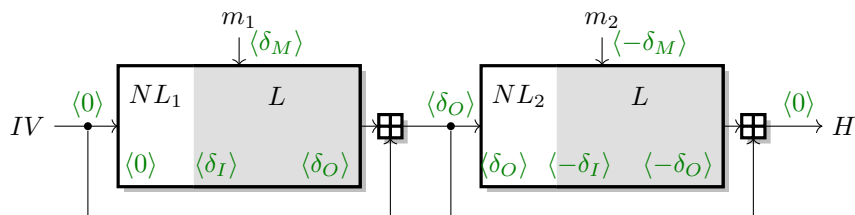


**Figure 1:** 2-block collision attack using a linear trail  $\delta_I \xrightarrow{\delta_M} \delta_O$  and two non-linear trails  $0 \rightsquigarrow \delta_I$  and  $\delta_O \rightsquigarrow -\delta_I$  in the first 10~15 steps. Green values between bracket represent differences in the state.

A huge breakthrough then happened in 2005: a team of researchers [29] showed that by generating non-linear differential trails (trails generated without linearizing the SHA-1 step function) for the first 10~15 steps of the compression function, one could potentially connect any incoming input difference to any fixed difference  $\delta_I$  at step 10~15. This flexibility allows to remove completely the impossibility issues one could face in the first steps due to the linearization (since this part is now non-linear). Even better, taking advantage of the Davies-Meyer construction used inside the compression function, it actually permits to perform the collision attack on SHA-1 using only two blocks containing differences, while picking the cheapest differential trail from step 10~15 to 80. With two successive blocks using the same differential trails (just ensuring that the output difference of the two blocks have opposite signs:  $0 \xrightarrow{\delta_M} \delta_O$  and  $\delta_O \xrightarrow{-\delta_M} -\delta_O$ ), one can see in Figure 1 that a collision is obtained at the end of the second block because the internal state differences cancel out.

### 2.2.2 Improving the Efficiency of Collision Search

Once the differential trail is set the attacker must find a pair of messages that follows it. A simple strategy uses an early-abort tree exploration for the 16 first steps, taking advantage of the degrees of freedom in the message, while the remaining steps are probabilistic. More advanced amortization methods (neutral bits [3], boomerangs [11, 10] or message modification [29]) are used to control more than 16 steps. Because of this amortization, usually the first 20 or so steps (which hold with a low probability because of the non-linear trail) do not contribute to the final complexity of the attack.

**Neutral bits** were first introduced for the cryptanalysis of SHA-0 [2, 3]. The idea is to find a small message modification (one or a few bits), that does not interact with necessary conditions in the differential path before a certain step  $x$ . Once a message pair following the differential path until step  $x$  is found, one can get another pair valid until step  $x$  by applying the modification. The probability that a modification is neutral until a step  $x$  can be pre-analysed before running the attack. A key observation is that any combination of two or more neutral bits until step  $x$  is likely to also be neutral until step  $x$ .

**Boomerangs [10] or tunnels [11]** are very similar amortization tools to neutral bits. Basically, they can be seen as neutral bits that are planned in advance. A perturbation built from one or a few local collisions (or relaxed versions) is neutral to the differential path after a few steps with a certain probability, but extra conditions are forced in the internal state and message to increase this probability. Boomerangs are generally more powerful than neutral bits (they can reach later steps than classical neutral bits), but consume more degrees of freedom. For this reason, only a few of them can be used, but their amortization gain is almost a factor 2.



Note that a lot of details have to be taken into account when using neutral bits or boomerangs, as many equations between internal state bits and message bits must be fulfilled in order for the differential path to be valid. Thus, they can only be placed at very particular bit positions and steps.

### 2.2.3 Chosen-prefix Collision Attacks

Chosen-prefix collision attacks are difficult to find for iterated hash functions such as SHA-1, because the attacker’s task is then to find a collision while starting from a random difference in the internal state (due to the prefixes pair that is not controlled at all by him). This random difference prevents to use directly the collision search techniques for SHA-1 aforementioned, because the attacker has to erase this random difference somehow and the interesting differential paths are in fact a very small set, where all output differences  $\delta_O$  only have a very low Hamming weight.

The first concrete application of a chosen-prefix collision attack was on MD5 [25] and this work was also the first to introduce a birthday search phase in order to partially avoid the random difference issue. The idea is to process random message blocks after the challenged prefixes, until the chaining variable difference  $\delta$  belongs to a large predetermined set  $\mathcal{S}$ . Since the message blocks after each prefix are chosen independently, this can be done with birthday complexity  $\sqrt{\pi \cdot 2^n / |\mathcal{S}|}$ . Then, from that difference  $\delta$ , one can reach a collision by slowly erasing the remaining unwanted difference bits by successfully applying some near-collision blocks (see Figure 2). We note that the starting difference set  $\mathcal{S}$  during the birthday phase must not be too small, otherwise this phase would be too costly. Moreover, the near-collisions blocks must not be too expensive either, and this will of course depend on the cryptanalysis advancements of the compression function being studied. This two-phase strategy was applied in [22] to the full SHA-1, for a cost of  $2^{77.1}$  hash calls. The improvement compared to the generic  $2^{80}$  attack is not very large, due to the difficulty for an attacker to generate enough allowable differences that can later be erased efficiently with a near-collision block, which makes the birthday part by far the most expensive phase of the attack. In [22] a set  $\mathcal{S}$  of 192 allowable differences was used, by starting from one type of near collision block and then varying the signs of the message and output differences, and also by letting some uncontrolled differences spread during the very last steps of the compression function.

This was improved in [12] by generalising for SHA-1 the set of possible differences that can be obtained for a cheap cost with a single message block, increasing the set size to 8768 elements. Another crucial improvement from [12] is the utilization of a multi-block strategy for SHA-1 that allows to further greatly increase the size of the set  $\mathcal{S}$ : the idea is that if an arbitrary input difference  $\delta_R$  can be decomposed as  $\delta_R = -(\delta_O^{(1)} + \delta_O^{(2)} + \dots + \delta_O^{(r)})$ , where each  $\delta_O^{(i)}$  can be reached as the output of a differential trail, the attacker just has to find near-collision blocks with output differences  $\delta_O^{(1)}, \dots, \delta_O^{(r)}$ , where each near-collision block will cancel one of the differences  $\delta_O^{(i)}$  composing  $\delta$  (see Figure 2). In particular, a clustering effect appears with this multi-block strategy, which can be leveraged by the attacker to select dynamically the allowable differences at the output of each successive block, to further reduce the attack complexity. This resulted in an estimated CP collision search complexity in the range of  $2^{66.9}$  to  $2^{69.4}$  hash evaluations, surprisingly not much greater than that of finding a simple collision.

## 3 Improving SHA-1 Collision Attack

Our first contribution is an improvement of the collision attack from Eurocrypt 2013 [22] and its GPU implementation from Crypto 2017 [23]. Through better use of degrees of freedom (message modifications and boomerangs) and code improvements, we gained a



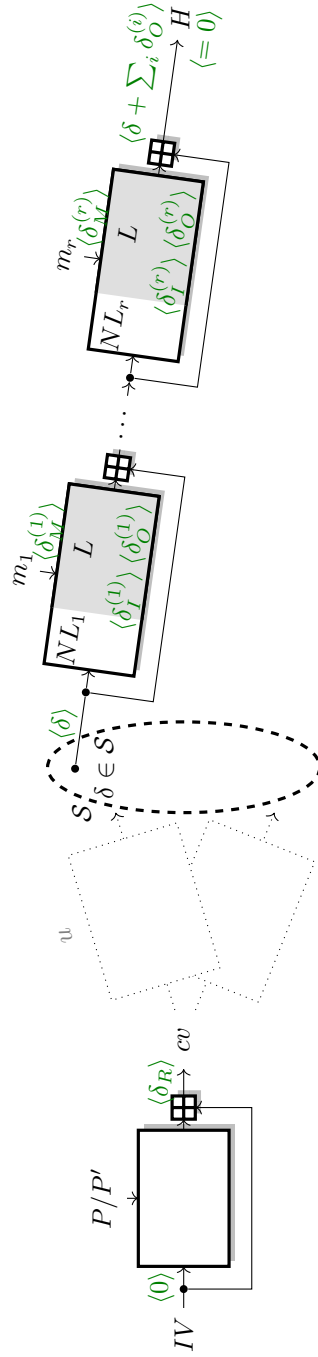


**Figure 2:** High-level view of a chosen-prefix collision attack. We assume that differences  $\delta \in S$  can be decomposed as  $\delta = -(\delta_O^{(1)} + \delta_O^{(2)} + \dots + \delta_O^{(r)})$ , where each  $\delta_O^{(i)}$  can be reached as the output of a differential trail.

factor between 8 and 10 (depending on GPU architecture) on the time needed to find a conforming block.

Since this part of our work is very technical, we only give an overview of our results in this section. Technical details can be found in Appendix A and the corresponding code is available at <https://github.com/SHA-mbles/sha1-cp>.

### 3.1 Analysis of Previous Works

First, we observed some differences between the theoretical analysis of [22] and the practical implementation of [23]. One of the boomerangs (on bit 6 of  $M_6$ ) contradicts one of the conditions used to maximize the probability of the path. Using this boomerang still improves the attack, because the gain in efficiency is larger than the loss in probability, but this affects the complexity evaluation. Similarly, one of the neutral bits used in the GPU code (on bit 11 of  $M_{13}$ ) contradicts another condition in the differential path, leading to an increase in complexity of a factor  $2^{0.2}$ .

In our analysis, we assume that the neutral bit on bit 11 of  $M_{13}$  is not used, and that the boomerang on bit 6 of  $M_6$  is only used for the last near-collision block, where the speed-up is most noticeable, and we have enough degrees of freedom to include all the boomerangs without difficulty. Therefore we can estimate more accurately the complexity of the previous CP attack [12] as  $2^{67.1}$  SHA-1 computations, instead of the range of  $2^{66.9}$  to  $2^{69.4}$  reported previously.

### 3.2 Additional Boomerangs

We found some additional boomerangs that can be used to speed-up the attack, on bits 4, 5, and 6 of  $M_{11}$ . Those boomerangs are not used in previous attacks because they interact badly with conditions of the differential trail, but this can be fixed by changing the last correction of the boomerangs to be a modular addition correction instead of an XOR correction.

More precisely, boomerangs are based on local collisions: an initial message difference introduces a difference in the state and another message difference cancels the state difference at a later step. In previous works, both message differences affect a single bit, so that they can be considered either as an XOR difference or as a modular difference. In this work, we only enforce a fixed modular difference for some boomerangs; depending on the value of the initial message, this difference will affect one or several bits (due to carries). Therefore, we can relax some of the conditions and make the additional boomerangs compatible with the differential path.

### 3.3 Precise Conditions of Neutral Bits

We also improved the rate of partial solutions generated by looking more precisely at the effect of each neutral bit. In particular, we found that some neutral bits flip with very high probability a certain condition after the step for which they are considered neutral. Therefore, these bits can be used as message modifications rather than neutral bits: instead of considering both the initial message and the message with the neutral bit applied and to test both of them at the later step, we can directly test the condition and decide which message to consider. Using this bit as message modification instead of neutral bit is more efficient, as one invalid branch in the search tree will be rightfully not explored.

In some cases, we also found that a bit that is neutral up to step  $i$  can only break some of the conditions of step  $i$ , while the rest will never be impacted. Therefore, we can test the conditions that are not affected before using that neutral bit, so as to avoid unnecessary computations. This strategy can be seen as a more precise neutral bit approach, where

**Table 4:** Cost of collision attacks. One collision requires on average  $2^{48.5}$   $A_{33}$ -solutions (those results include the boomerang on  $M_6[8]$ ).

Note: we use the hashrate from hashcat, which is slightly over-optimistic (i.e. attack cost in SHA-1 computations is overestimated).

GPU	arch	Hashrate	Collision (old)		Collision (new)		Gain
			$A_{33}$ rate	SHA-1	$A_{33}$ rate ( $r$ )	SHA-1	
K20x (1 GPU)	Kepler	1.7GH/s	28k/s	$2^{64.4}$	255k/s	$2^{61.2}$	9.1
GTX 970	Maxwell	3.9GH/s	59k/s	$2^{64.5}$	570k/s	$2^{61.2}$	9.6
GTX 1060	Pascal	4.0GH/s	53k/s	$2^{64.7}$	470k/s	$2^{61.6}$	8.8
GTX 1080 Ti	Pascal	12.8GH/s	170k/s	$2^{64.7}$	1500k/s	$2^{61.6}$	8.8

the attacker doesn't work step-wise, but instead condition-wise: more fine-grained filtering will lead to computation savings.

All in all, these tricks result in a better exploration of the collision search tree by cutting branches earlier. We give detailed benchmarks results and complexity estimates in Table 4, after implementing our improvements in the code of [23] (where an  $A_i$ -solution refers to an input pair that is following the differential path until word  $A_i$  inclusive).

### 3.4 Building Differential Trails

Following [12], we try to reuse as much as possible the previous works on SHA-1, and to keep our differential trail as close as possible to the attack of Stevens *et al.* [23], out of simplicity. More precisely, for each block of the collision phase, as starting point we reused exactly the same core differential path as in [23]: the difference positions in the message are the same, and the difference positions in the internal state are the same after the first 13 steps (roughly). We also tried to keep difference signs to be the same as much as possible. However, we made some modifications to the boomerangs and neutral bits as explained in the previous subsection.

The starting path skeleton is depicted in Figure 3. For each new block of the near-collision phase, we:

1. collect the incoming chaining variable and its differences and insert them inside the skeleton;
2. set the signs of the differences in the very last steps (chosen so as to minimize the final collision complexity according to the graph, see Section 4) and generate the linear system of all equations regarding the message words;
3. compute a valid non-linear differential path for the first steps;
4. generate base solutions, *i.e.* partial solutions up to  $A_{14}$ , possibly using help of neutral bits;
5. from the base solutions, search for a pair of messages that fulfils the entire differential path, using neutral bits, message modifications and boomerangs.

Steps 1 to 4 are done on CPU because they are not too computationally intensive, but step 5 runs on GPU.

We observe that in comparison with the classical collision attack [23], we have fewer degrees of freedom available in our differential paths, due to slightly more linear constraints we imposed on the late-step message bits. Moreover, for the first blocks of the near-collision phase, the attacker will have to handle a denser input difference on the chaining variable, which will render the non-linear part search a little more difficult and little more consuming in terms of freedom degrees. In any cases, we had enough degrees of freedom to find a conforming messages pair for all blocks during the attack.

$i$	$A_i$	$W_i$
-4:		
-3:		
-2:	Incoming Chaining Variable	
-1:		
00:		---xx-----x-
01:	?????????????????????????????????????--	xx-----x-
02:	???????????????????????????????????????	x-xx-x-----xxx--
03:	???????????????????????????????????????	--xxxx-----x-
04:	???????????????????????????????????????	x-xxxx-----xx-x-
05:	????????????????????????????????????? ? ?????????	-x-----x-
06:	????????????????????????????????????? ? ?????????	--x-x-----0-0-xxx--
07:	???-----0-0?????	xxx-xx-----1-1-----x-x-
08:	???x----- -0?0--??	---xx-----x-
09:	???----- -1?1--??	xx-----0-x-
10:	???----- 0 ?---??	x-xx-x-----1-----xxx--
11:	?x----- 0 0----	-x-xx-----111-x-
12:	-----111----	x-xxux-----xx--
13:	n-----000--	x-xx-----1u--
14:	--n-----111--	-----1-xx--
15:	u-1-1-----	x-xxx-----n--
16:	un0-0-----	--u-----nu--
17:	u--1-----	-xxnn-----n--
18:	u-u0-----	--0-n-----n-n--
19:	u-----	-xuu-----n--
20:	u-u-----	x-nux-----nnu--

**Figure 3:** Skeleton of starting differential path for all blocks during the near-collision phase of our CP collision attack on SHA-1 (only the first 20 steps are depicted). The MSB's are on the right and “-” stands for no constraint, while the notation “|” on two bits vertically adjacent mean that these two bits must be equal. The other notations are similar to the ones used in [7]. This is only to give a general idea of the differential path used, as several conditions on the message and/or on the internal state are not represented here.

We also remark that the incorporation of the additional short boomerangs reduces the number of neutral bits that can be used in comparison to [23]. Yet, this was not an issue as we still had enough to keep the GPU busy (in stage 5) while the CPU was producing the base solutions (in stage 4), even though our computation cluster is composed of low range CPUs.

## 4 Improving SHA-1 CP Collision Attack

In order to take advantage of the low-level improvements to collision attack techniques, we must also improve the high-level chosen-prefix collision attack.

The complexity of the birthday phase depends on the size of the set  $\mathcal{S}$  of differences that can be erased from the state, therefore we need a larger set. For the near-collision phase, the complexity depends on how we combine the near-collision blocks to erase the difference in the state. We improve the graph techniques of [12] and suggest a more heuristic approach, resulting in a lower average complexity, but without a guaranteed upper bound.

### 4.1 Graph Construction

In order to efficiently erase the differences from the set  $\mathcal{S}$ , [12] uses a graph where vertices are the state difference in  $\mathcal{S}$ , and there is an edge between  $\delta$  and  $\delta'$  if  $\delta' - \delta$  can be obtained as the output difference of the compression function (using a near-collision block). The birthday phase designates a starting node in the graph and we just have to follow a path leading to the zero difference, as illustrated in Figure 4. For each edge, we search for

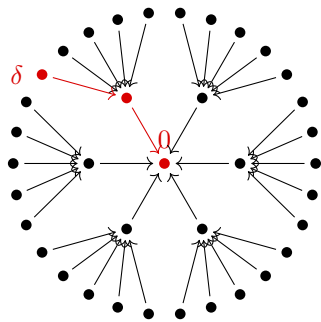


Figure 4: Graph search.

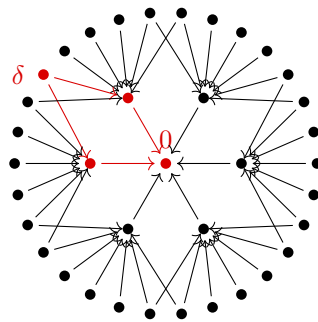


Figure 5: With clustering.

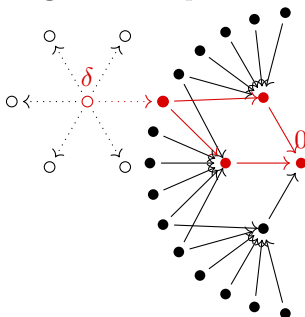


Figure 6: Bi-directional.

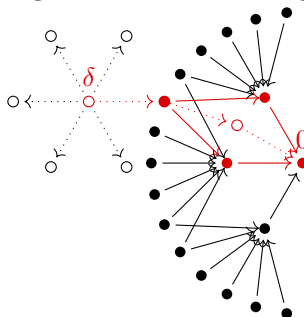


Figure 7: Implicit.

a block with the correct output difference, using near-collision search, with a cost that depends on the target difference. In the following, we denote the cost for the optimal output differences as  $C_{\text{block}}$ ; it is equivalent to the cost of an identical-prefix collision.

**Large graph.** We started with the same approach as in [12], building a series of graphs with increasing limits on the number of blocks allowed. More precisely, we consider the set of all nodes that are reachable with a path of cost at most  $24 C_{\text{block}}$  and up to 10 blocks. This results in a graph with  $2^{36.2}$  nodes<sup>1</sup>, which requires 2TB of storage (storing only the nodes and their cost).

**Clustering.** In order to minimize the complexity of the near-collision phase of the attack, [12] uses a clustering technique to exploit multiple paths in the graph (see Figure 5). Indeed, the near-collision search does not have to commit to a fixed output difference. When two output differences correspond to useful paths in the graph and are compatible with the same differential path, the attacker can run the near-collision search and stop as soon as one of them is obtained.

Concretely, let us assume we have two output differences  $\delta_1$  and  $\delta_2$  compatible with the same differential trail, that can each be reached with a cost of  $C_{\text{block}}$ . There are two different ways to erase a difference  $-\delta_1 - \delta_2$  in the state:

- a block with difference  $\delta_1$ , followed by a block with difference  $\delta_2$ ;
- a block with difference  $\delta_2$ , followed by a block with difference  $\delta_1$ .

If we don't decide in advance the target difference for the first block, the search is expected to reach either  $\delta_1$  or  $\delta_2$  with a cost of only  $0.5 C_{\text{block}}$ , leading to an attack complexity of  $1.5 C_{\text{block}}$  rather than  $2 C_{\text{block}}$ .

<sup>1</sup>The largest graph suggested in [12] has size  $2^{33.7}$ .

**Table 5:** Size of the set  $\mathcal{S}$  with various limits on the maximum cost and on the number of near-collision blocks ( $\log_2$ ).

Max Cost	1 bl.	2 bl.	3 bl.	4 bl.	5 bl.	6 bl.	7 bl.	8 bl.	9 bl.	10 bl.
1 $C_{\text{block}}$	8.17	8.17	8.17	8.17	8.17	8.17	8.17	8.17	8.17	8.17
2 $C_{\text{block}}$	9.17	16.30	19.92	22.05	23.13	23.95	24.44	24.55	24.62	24.65
3 $C_{\text{block}}$	10.17	17.10	21.76	24.66	26.58	27.95	28.96	29.71	30.31	30.76
4 $C_{\text{block}}$	12.53	18.60	22.97	26.34	28.68	30.35	31.56	32.54	33.29	33.88
5 $C_{\text{block}}$	12.53	19.65	24.18	27.44	29.83	31.65	33.04	34.14	34.90	35.42
6 $C_{\text{block}}$	12.53	19.79	24.81	28.26	30.74	32.62	34.05	35.08	35.67	36.03
7 $C_{\text{block}}$	13.09	20.37	25.30	28.82	31.35	33.24	34.59	35.43	35.86	36.15
8 $C_{\text{block}}$	13.09	20.62	25.72	29.27	31.81	33.65	34.81	35.54	35.92	36.19

In our case, we initially consider nodes at distance up to  $24 C_{\text{block}}$  and we run the clustering technique to get a better estimate of the complexity when we don't specify in advance the sequence of differences. After several weeks of computation on a machine with 48 cores and 3TB of RAM, we find that almost 90% of the nodes are actually at distance  $6 C_{\text{block}}$  or less, as seen in Table 5.

All the differences in this set are active only on a 64-bit mask. Therefore, we use those bit positions for the birthday phase: we truncate SHA-1 to the remaining 96 bits<sup>2</sup> and we generate a large number of partial collisions until one of them corresponds to a difference in the graph.

## 4.2 Bi-directional Graph

Since the CP collision attack is essentially a path search in a graph, we can use a bi-directional search to make the search more efficient. More precisely, when we evaluate the cost of a node, instead of just looking it up in the graph, we recompute all edges starting from the node to see if they reach the graph and compute the cost using the clustering formula. This corresponds to a bi-directional search where we pre-compute in the backwards direction the set of values that go to zero after at most 10 blocks, and during the online phase, we compute one block forward. This is illustrated by Figure 6, where black dots correspond to precomputed nodes stored in the graph, and white dots are only computed during the online phase.

This can be seen as a time-memory trade-off: we use nodes at a distance up to 11 blocks, but we only build explicitly the graph with 10 blocks. Moreover, we can use nodes that are not reachable with a single trail of cost below  $24 C_{\text{block}}$ , and that are therefore excluded from our initial graph. Indeed, if there exists a trail such that the cost is below  $24 C_{\text{block}}$  when removing an edge, the forward search using that edge will hit the explicit graph, and we can evaluate the distance of the node.

We can't compute exactly the size of this implicit graph, but we can evaluate it experimentally by simulating the birthday phase of the attack. We found that we need on average  $2^{26.4}$  attempts before hitting the graph, which corresponds to a graph size of roughly  $2^{38}$  (assuming that we detect being in the graph with a probability of 0.75, as was the case with the parameters of [12]).

## 4.3 Implicit Nodes

Following [12], we build the graph using a set  $\mathcal{D}$  of 8768 potential output differences with high probability (corresponding to a cost up to  $8 C_{\text{block}}$ ). However, there are many other

<sup>2</sup>Given by mask 0x7f000000, 0xffff80001, 0x7ffff000, 0x7fffffc0, 0x7ffffff

output differences that can be useful in our attack, even if they have a lower probability: we can use a block as long as the new state difference gets closer to a collision. Therefore, during the near-collision phase, instead of keeping only blocks with an output difference corresponding to an explicit edge of the graph, we keep all blocks that follow the trail up to step 61 and we look up the new state difference in the graph (using the bi-directional strategy above). With a larger number of usable output differences, the cost of each block decreases (Figure 7).

Again, we can't compute explicitly the complexity of this attack strategy, but we can run simulations. According to our experiments with the graph described above, the average cost of the near-collision phase is only  $2 C_{\text{block}}$ , even though most of the nodes in the graph correspond to a cost of  $6 C_{\text{block}}$  when following edges that have been explicitly considered.

Finally, we can use this strategy to reduce the number of near-collision blocks used in the attack. In practice, we observed that most of the nodes in our graph can actually be reached with fewer than 11 blocks. In particular, when using output differences that do not correspond to edges of the graph, we often reach an output difference that can be erased with fewer blocks than expected, in particular for the first near-collision blocks.

## 5 Chosen-Prefix Collision Computation

Even though we managed to reduce the cost of the chosen-prefix collision for **SHA-1** to only  $2^{63.7}$  **SHA-1** evaluations, performing such a large-scale computation remains very expensive. We show that it can be computed with an academic budget, for a total cost much lower than US\$ 100k.

### 5.1 Attack Parameters

Using more blocks for the near-collision blocks part of the attack leads to improved attack complexity, but one can observe that the improvement becomes marginal as the number of block increases. Besides, in order to allow for a practical real-life use of our chosen-prefix collision (see next section), we had to enforce a limit on the total number of blocks.

Using the idea described in the previous section, we have the following parameters for the attack:

- We use a limit of at most 11 blocks, but we aim for 10 blocks at most for the attack (to fit in a 6144-bit key, see next section);
- The graph  $\mathcal{G}$  has size roughly  $2^{38}$ , but it is not computed explicitly;
- The birthday stage is a parallel collision search algorithm (using the distinguished points technique of [28]) with a mask of 96 bits, and we need about  $2^{26.4}$  partial collisions on those 96 bits. Therefore the expected complexity of the birthday phase is  $\sqrt{\pi 2^{96} 2^{26.4}} \approx 2^{62}$ ;
- We use chains (consecutive iterations of the function from a starting point during the distinguished points technique) of length  $2^{28}$ , resulting in a data complexity of  $1/2$  TB to store  $2^{34}$  chains;
- We expect a cost of  $2 C_{\text{block}}$  for the near-collision phase.

In hindsight, we could have use longer chains to reduce the data storage, and to make sorting the data on our cluster easier. We could also have aimed for a lower number of blocks: our collision used only 9 blocks, and we could probably reach 8 or 7 without much impact on the complexity.

**Complexity estimate.** Overall, for the attack parameters chosen, the birthday part costs about  $2^{62.05}$  **SHA-1** computations, while the near-collision part is expected to require  $1 C_{\text{block}}$  for the last block, and  $1 C_{\text{block}}$  in total for the previous blocks.



As explained in Section A.1, we use the boomerang on  $M_6[8]$  for the last block, so that the expected time to find a conforming block can be estimated directly from the figures of Table 4 as  $C_{\text{block}} = 2^{48.5}/r$ . For the intermediate blocks, we don't use this boomerang, so the rate is reduced to  $r/1.9$  but we only require  $2^{48.08}$   $A_{33}$ -solutions for one  $C_{\text{block}}$ . Our simulations show that the total cost for all intermediate blocks is roughly one  $C_{\text{block}}$ , therefore it will take time  $C_{\text{block}} = 1.9 \cdot 2^{48.08}/r$ . Finally, we can estimate the total attack time as

$$2^{62.05} \cdot h + \frac{2^{48.5} + 1.9 \cdot 2^{48.08}}{r},$$

with  $r$  the  $A_{33}$ -solution rate (from Table 4), and  $h$  the hash-rate for the birthday phase (from Section 5.3). We give concrete complexity estimates on several GPUs in Table 2. Our chosen-prefix collision attack is roughly four times as expensive as an identical-prefix attack.

## 5.2 A GPU Cluster

We originally estimated that our attack would cost around US\$ 160k by renting GPUs from a cloud provider such as Amazon or Google (using spot or preemptible prices). However, since our computations do not need much communication between the GPUs, nor fancy inter-GPU task scheduling, we can consider renting cheaper GPUs from providers that use gaming or mining cards in consumer-grade PCs, rather than the datacenter-grade hardware used by big cloud providers. Services like [gpusersrental.com](https://www.gpuserversrental.com) rent GTX 1060 or GTX 1080 GPUs for a price below 5 cents per month per CUDA core; which would give a total cost around US\$ 75k to compute a chosen-prefix collision.

After some cost analysis, we have concluded that GTX 1060 GPUs offered a very good hashrate/cost ratio at the time of the chosen-prefix collision computation. GPU prices vary significantly depending on cryptocurrency prices, but at the time of writing, a GTX 1060 can be rented for about US\$ 35 per month<sup>3</sup>. Our attack requires about 107 GPU-years using GTX 1060, which gives an estimated cost of  $107 \times 35 \times 12 \simeq$  US\$ 45k to compute a chosen-prefix collision for SHA-1.

Our cluster was made of 150 machines with 6 GPU each (with a mix of GTX 1060 3G, and GTX 1060 6G), and one master node with two 2TB hard drives in a RAID configuration. The master node had a Core i7 CPU, but the GPU nodes had low-end Pentium or Celeron CPU with two cores. Each machine ran Ubuntu Linux, but there was no cluster management software installed (we used `cflush` to run commands on all the nodes). We negotiated a price of US\$ 37.8k per month (higher than current prices), and used the cluster for two months.

**Cost analysis.** We paid US\$ 75.6k for our computation, but the cost could be as low as US\$ 50k with currently lower GPU prices and less idle time. With the same methods, computing an identical-prefix SHA-1 collision would cost only about US\$ 11k. This is clearly within reach of reasonable attackers.

Of course the underlying weakness of SHA-1 has always been present, even if it was not public (and maybe not discovered). We estimate that a PS3 cluster (as used by Stevens et al. [27], and as deployed by the US army<sup>4</sup>) could have implemented this attack for a cost of a few million dollars in 2010, when SHA-1 was still the most widely used hash function. This underlines that the depreciation process of SHA-1 should have been much faster after the publication of the first theoretical collision attack in 2004.

<sup>3</sup>More precisely, US\$ 209 per month for 6 GTX 1060 3GB: <https://web.archive.org/web/20191229164814/https://www.gpuserversrental.com/>

<sup>4</sup><https://phys.org/news/2010-12-air-playstation-3s-supercomputer.html>

**Table 6:** Timeline of the birthday phase.

Date	Event	Complexity	# collisions
July 25	Starting cluster setup		
July 27	Computation started		
August 14	Step 2 unsuccessful	$2^{61.9}$	$2^{25.8}$
August 20	Step 2 unsuccessful	$2^{62.4}$	$2^{26.6}$
August 24	Step 2 unsuccessful	$2^{62.6}$	$2^{27.1}$
August 30	Step 2 successful!	$2^{62.9}$	$2^{27.7}$

Looking at the future, this attack will get even cheaper as computation costs decrease. Following Moore’s law (that seems to be still valid for GPU<sup>5</sup>), we estimate that it should cost less than US\$10k to generate a SHA-1 chosen-prefix collision by 2025.

### 5.3 Birthday Phase

In order to simplify the implementation, we implemented the birthday phase with two distinct steps: in the first step, each GPU computes independently a series of chains, and in the second step we gather all the results, sort them to find collisions in the end-points, and re-run the chain to locate the collisions. Our implementation runs at a speed of  $h = 3.5\text{GH/s}$  on GTX 1060 GPUs (respectively  $3.2\text{ GH/s}$  on GTX 970 and  $11\text{ GH/s}$  on GTX 1080 Ti). This is somewhat lower than the hashcat benchmarks reported in Table 2 because hashcat can skip some parts of SHA-1, and we have to keep two SHA-1 states in the registers to implement the birthday phase. Every time we run the second step, we then search the collisions in the graph, to determine whether we have reached a useful starting point (this is run on a separate machine with at least 1TB of RAM, and we let the cluster restart the first step in the meantime).

As shown in Table 6, we ran step 2 four times, and we have been quite unlucky in the birthday phase, only succeeded after finding  $2^{27.7}$  collisions, rather than the estimated  $2^{26.4}$ . It took us 34 days to compute those chains, which corresponds to a hashrate  $2.9\text{ TH/s}$  for our cluster (including downtime).

Interestingly, we got slightly fewer collisions than expected (after a given number of chains): we expected to compute  $\sqrt{\pi 2^{96} C}$  SHA-1 to find  $C$  partial collisions, but our analysis is off by a factor roughly  $2^{0.2}$ . Given the small magnitude of the error, we didn’t investigate further, but it could be due to an unknown bug in our code, or an issue in the analysis (such as a failed independence assumption, or an issue with chains that reach a cycle).

### 5.4 Near-collision Phase

The near-collision phase is very technical and very complex. Every time a block is found, we have to prepare the search for the next block. This first requires to traverse the graph  $\mathcal{G}$  to find the parameters for the next block: we have different constraints in the last steps depending on which output differences are desired. Then, we had to generate a new non-linear part for the early steps, as explained in Section 3.4. We used tools similar to [7], which take a lot of parametrization and trial-and-error to have a proper non-linear part that fits nicely with the core differential path. Finally, some testing and configuration of the GPU code was then required to check how neutral bits and boomerangs behaved in this new configuration. In particular, there were usually some adjustments to make in the

<sup>5</sup><https://blogs.nvidia.com/blog/2017/05/10/nvidia-accelerates-ai-launches-volta-dgx-workstation-robot-simulator-more/>

**Table 7:** Timeline of the near-collision phase.  $C_{\text{block}}$  corresponds to  $2^{19.17}$   $A_{61}$ -solutions, excepted for the last block where the use of an extra boomerang increases it to  $2^{19.58}$

Date	Event	$\#A_{61}\text{-sol}$	Complexity
September 07	Block 1 found <sup>a</sup>	$2^{16}$	0.11 $C_{\text{block}}$
September 09	Block 2 found	$2^{13.5}$	0.02 $C_{\text{block}}$
September 13	Block 3 found	$2^{16.9}$	0.21 $C_{\text{block}}$
September 14	Block 4 found	$2^{10.8}$	0.003 $C_{\text{block}}$
September 16	Block 5 found	$2^{15.5}$	0.08 $C_{\text{block}}$
September 18	Block 6 found	$2^{15.5}$	0.08 $C_{\text{block}}$
September 20	Block 7 found	$2^{16}$	0.11 $C_{\text{block}}$
September 21	Block 8 found	$2^{14.5}$	0.04 $C_{\text{block}}$
September 27	Block 9 found <sup>b</sup>	$2^{18.2}$	0.38 $C_{\text{block}}$

<sup>a</sup>Two solutions found

<sup>b</sup>Using the  $M_6[8]$  boomerang

GPU code for the more complex conditions in the path that involve several bit positions. The entire preparation process would have potentially to be performed again in case of any issue detected with the path found.

This was automated to some extent, but still took between a few hours and a few days of manual work to prepare for each block (it took more time for the first blocks because there are more constraints to build the path, and we were more experienced for the later blocks). Unfortunately, this means that the GPU cluster was not doing useful work during this time. We remark that our attack could have cost less if we had fully automated the entire cryptanalysis process, or if we had improved the search algorithm for the non-linear part of the differential path. This is definitely not impossible to achieve, but it would require a lot of tedious work.

For the last block, we started the computation without the boomerang on  $M_6[8]$ , and modified the path and the code after one day to include it. As explained in Section 3, this extra boomerang reduces the quality of  $A_{61}$ -solutions, so that we need  $4/3$  times the number of solutions ( $2^{19.58}$  instead of  $2^{19.17}$ ), but it almost doubles the production rate of these solutions. In total, this reduces the computation time by a factor  $1.9/4/3 \approx 1.4$ .

As expected, intermediate blocks cost much less than  $C_{\text{block}}$  (the cost of a block with a pre-determined output difference) because we can target a large number of output differences. Only the last block is expected to cost  $C_{\text{block}}$ . However, we were quite lucky in this phase of attack, because we found all the blocks after only  $0.9 C_{\text{block}}$ , rather than the estimated  $2 C_{\text{block}}$ . In particular, the last block was found after only  $2^{18.2}$   $A_{61}$ -solutions ( $0.38 C_{\text{block}}$ ), instead of the expected  $2^{19.58}$ .

A timeline of the near-collision phase is given in Table 7, and the chosen-prefix collision is given in Appendix B (with the actual messages in Figure 13 and the intermediate differences in Table 9).

## 5.5 Resources Used

A quick overview of the resources used for each part is given in Table 8. If we evaluate the total useful GPU time spent for the attack, we have roughly:

- 78 years for the birthday phase
- 25 years for blocks 1 to 9
- 10 years for the last block

**Table 8:** Resources used for the attack

Phase	Step	Main resource	Repetitions	Wall time
Setup	Preparation of the graph	CPU and RAM		≈ 1 month
Birthday	Computing chains	GPU		34 days
	Sorting chains	Hard drive	4 ×	≈ 1 day
	Locating collisions	GPU	4 ×	< 1/2 day
	Searching in graph	RAM	4 ×	< 1/2 day
Blocks	Building trail & code	Human Time	9 ×	≈ 1 day
	Finding block	GPU	8 ×	3 hours – 3 days
	Checking results in graph	RAM	8 ×	< 1/2 hour
	Finding last block	GPU	1 ×	6 days

This means that roughly 75% of our GPU time was useful. If we convert the attack time to **SHA-1** evaluations, we arrive at a total of  $2^{63.6}$ , which is quite close to the estimate of  $2^{63.5}$  given in [Table 2](#).

## 6 Application to PGP Web of Trust

Our demonstration of a chosen-prefix collision targets the PGP/GnuPG Web of Trust. This trust model relies on users signing each other’s identity certificate, instead of using a central PKI. For compatibility reasons the legacy branch of GnuPG (version 1.4) still uses **SHA-1** by default to sign identity certificates.

Therefore, we can impersonate a user using a **SHA-1** chosen-prefix collision to forge the signature. More precisely, our goal is to create two PGP keys with different UserIDs, so that key B is a legitimate key for Bob (to be signed by the Web of Trust), but the signature can be transferred to key A which is a forged key with Alice’s ID. This will succeed if the hash values of the identity certificates collide, as in previous attacks against X.509 MD5-based certificates [25, 27]. Moreover, due to details of the PGP/GnuPG certificate structure, our attack can reuse a single collision to target arbitrary users Alice and Bob: for each victim, the attacker only needs to create a new key embedding the collision, and to collect a **SHA-1** signature. This is arguably the first practical attack against a real world security application using weaknesses of **SHA-1**.

We recall that a chosen-prefix collision attack works as follows: given two arbitrary prefixes  $P$  and  $P'$ , an attacker can generate two messages  $M$  and  $M'$  such that  $H(P \parallel M) = H(P' \parallel M')$ . Note that in classical iterated hash functions such as **SHA-1**, given an arbitrary suffix  $X$ , we still have  $H(P \parallel M \parallel X) = H(P' \parallel M' \parallel X)$ .

### 6.1 Exploiting a Chosen-prefix Collision

We now focus on the identity certificates that will be hashed and signed. Following RFC 4880 [5], the hash computation done during certificate signing receives the public key packet, then a UserID or user attribute packet, and finally a signature packet and a trailer. The idea of the attack is to build two public keys of different sizes, so that the remaining fields to be signed are misaligned, and we can hide the UserID of key A in another field of key B. Following RFC 4880, the signature packet is protected by a length value at the beginning *and at the end*, so that we have to use the same signature packet in key A and key B (we cannot stuff data in the hashed subpacket). Therefore, we can only play with the UserID and/or user attribute packets. Still, a user attribute packet with a JPEG image gives us enough freedom to build colliding certificates, because typical JPEG readers

ignore any bytes after the End of Image marker (`ff d9`). This gives us some freedom to stuff arbitrary data in the certificate.

More precisely, we build keys A and B as follows. Key A contains an 8192-bit RSA public key, and a UserID field corresponding to Alice. On the other hand, key B contains a 6144-bit RSA public key, the UserID of Bob and a JPEG image. Therefore, when Bob gets a certification signature of his key, the signer will sign two certificates: one containing his public key and UserID, and another one containing the public key and the image. The public keys A and B and the image are crafted in such a way to generate a collision between the certificates with the key A and Alice's UserID, and the certificate with key B and the image.

### 6.1.1 Content of Identity Certificates

Figure 8 shows a template of the values included in the identity certificate: those values are hashed when signing a key, and we want the two hashes to collide. In this example, the UserID field of key A contains "Alice <alice@example.com>", and the image in key B is a valid JPEG image that will be padded with junk data after the End of Image marker. The real JPEG file is 181 bytes long<sup>6</sup> (from `ff d8` to `ff d9`), and it is padded with 81 bytes, so that the file included in the key is 262 bytes long (here the padding includes 46 bytes corresponding to the end of the modulus of key A, 5 bytes corresponding to the exponent of key A, and 30 bytes corresponding to Alice's UserID).

In Figure 8, we use the following symbols:

- 01 Bytes with a fixed value are fixed by the specifications, or chosen in advance by the attacker (length of fields, UserID, user attribute, ...)
- ?? Represent bytes that are determined by the chosen-prefix collision algorithm (the messages  $M$  and  $M'$  to generate a collision)
- !! Represent bytes that are selected after finding the collision, to generate an RSA modulus with known prime factors
- .. Represent bytes that are copied from the other certificate
- \*\* Represent time-stamps chosen by the attacker
- \$\$ Represent the time-stamp chosen by the signer

Underlined values correspond to packet headers (type and length).

### 6.1.2 Attack Procedure

To carry out the attack, we have to perform the following steps:

1. Build a chosen-prefix collision with prefixes "99 04 0d 04 \*\* \*\* \*\* \*\* 01 20 00" and "99 03 0d 04 \*\* \*\* \*\* \*\* 01 18 00", after filling the **\*\*** with two arbitrary time-stamps. The chosen-prefix collision must have at most 10 near-collision blocks. This determines the **??** bytes of the keys.
2. Choose a tiny JPEG image to include in key B (fixed orange bytes), and an arbitrary UserID to include in key A (fixed yellow bytes)
3. Select "**!!**" bytes in B to obtain a modulus with known factors
4. Select "**!!**" bytes in A to obtain a modulus with known factors
5. Generate key B with the modulus and the padded JPEG. Ask for a signature of the key.
6. Copy the signature to key A.

We point out that the chosen-prefix collision is computed *before* choosing the UserIDs and images that will be used in the attack. Therefore, a single CPC can be reused to

<sup>6</sup>Building a JPEG image smaller than 256 bytes is not easy, but it is possible

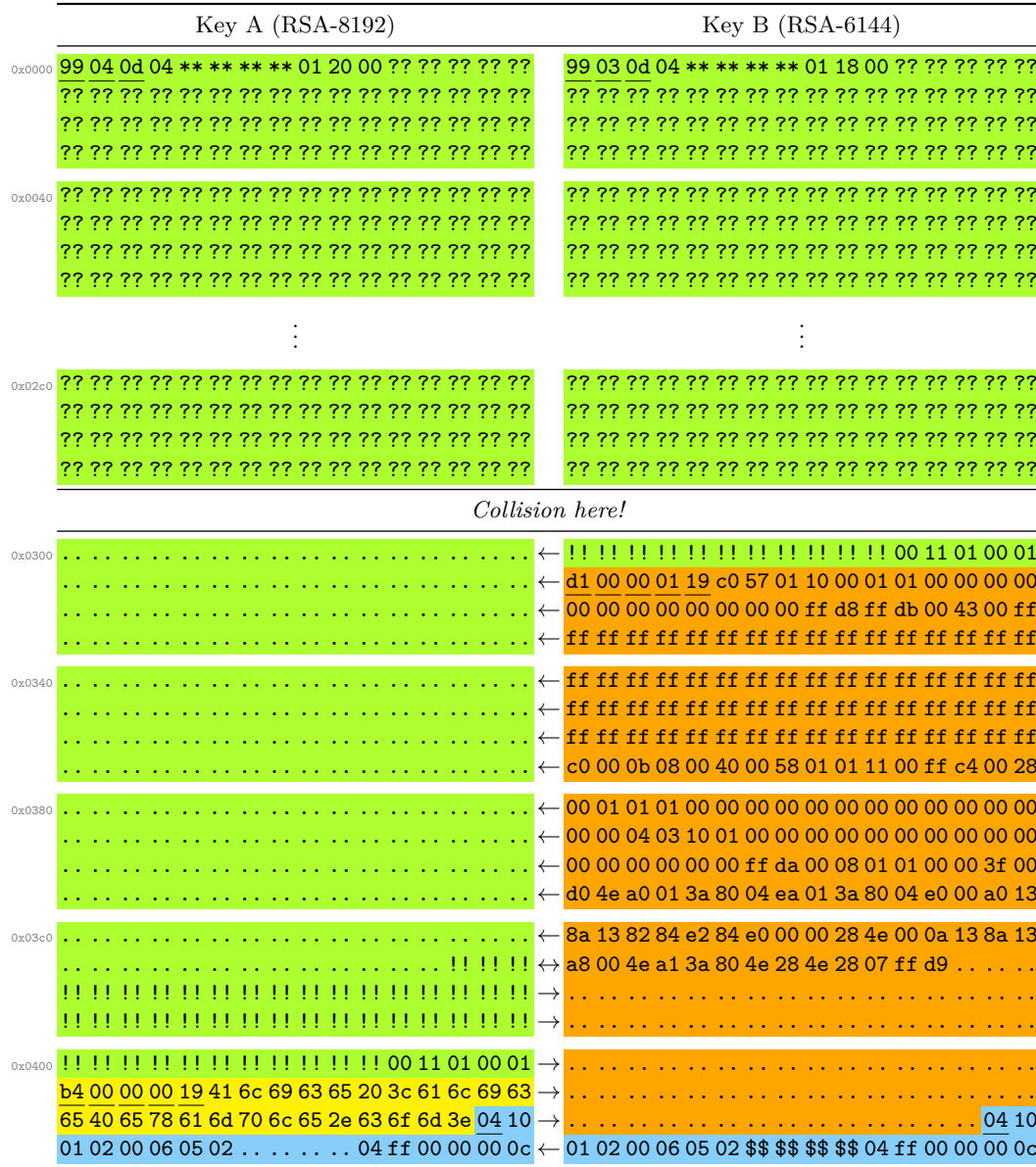


**Figure 8:** Construction of colliding OpenPGP identity certificates. The colour corresponds to the packets hashed when computing the signature: first, the public key packet (with header), then the UserID or user attribute, and finally the signature packet and trailer. Arrows show when a value is chosen in one key and copied to the other.

attack many different victims. This contrasts with attacks on X.509 certificates [25, 27], where the identifier is hashed before the public key.

In order to build the modulus (steps 3 and 4 above), we use the same strategy as in previous works [25, 27]. More precisely, the high order bits are fixed by previous steps, and the low-order bits can be chosen freely. Therefore we have to find a modulus in an interval  $[A, B]$  with a known factorisation. We select a random prime  $P$  (in the order of  $B - A$ ), and we compute  $Q = \lfloor B/P \rfloor$ . If  $Q$  is a prime, we use  $P * Q$  as the modulus: we have  $A \leq P * Q \leq B$  when  $P \leq B - A + 1$ . This takes a few minutes in practice.

We note that the factors of the modulus are unbalanced. With the template of Figure 8, we expect factors of 88 bits and 6056 bits for Key B, and 368 bits and 7824 bits for key A. In practice we managed to find a CP collision with fewer blocks than in Figure 8, so that key B actually has factors of 1112 bits and 5032 bits. This makes both keys hard to factor. As mentioned in [14], it is possible to find modulus with somewhat larger factors using more advanced techniques.

### 6.1.3 Example Keys

We show an example of a pair of keys generated with this procedure in Figures 11 and 12 from the Appendix. The keys can be examined with `pgpdump -i` to see that they include the same signature. The files can be directly downloaded from these URLs:

**Key A:** <https://SHA-mbles.github.io/alice.asc>

**Key B:** <https://SHA-mbles.github.io/bob.asc>

In our demonstration, we chose a time-stamp far in the future to avoid malicious usage of our collision. However, an attacker that can repeat our work will obviously use a valid time-stamp.

### 6.1.4 Attack Variant

We also found an alternative attack, exploiting the PGP key format in a slightly different way, where key B contains a short public key followed by a JPEG image. We would consider both the public key and the image as the prefix, and stuff the CPC blocks inside the image (after the EOI marker). This variant leaves a smaller space for the CPC blocks, but the advantage is that key A is less suspicious because it doesn't need to contain a valid JPEG file inside the modulus (the modulus is really made of random-looking blocks). On the other hand, this variant requires to compute a new CPC for each key B.

Other variants might also be possible.

## 6.2 Impact

As explained in Section 7.1, the “classic” branch of GnuPG (v1.4) uses SHA-1 by default for identity certifications, and there is still a non-negligible number of keys signed with SHA-1. Before our attack was disclosed, SHA-1 signatures were also accepted by the “modern” branch of GnuPG (v2.2). This made the attack usable in practice.

In addition, a single CPC can be reused to attack many different victims, so that the cost of the CPC is just a one-off cost. Given our cost estimation around US\$ 50k, this is well within reach of strong adversaries.

## 7 SHA-1 Usage and Disclosure

SHA-1 is still used in a surprising number of security applications. It is supported in many secure channel protocols (TLS, SSH), and remains actually used for some fraction of the



connections. It is also used for PGP identity certifications, and it is the foundation of GIT versioning system. We expect there are also an important number of proprietary systems using `SHA-1`, but getting actual data on this is difficult.

Collisions and chosen-prefix collisions do not threaten all those usages (in particular `HMAC-SHA-1` seems relatively safe), but there are several settings that are directly affected by chosen-prefix collisions:

- PGP identities can be impersonated if trusted third parties sign identity certificates with `SHA-1` (see 7.1)
- X.509 certificates could be broken if some CAs issue `SHA-1` certificates with predictable serial numbers (see 7.2)
- TLS and SSH connections using `SHA-1` signatures to authenticate the handshake could be attacked with the SLOTH attack [1] if the CP collision can be generated extremely quickly (see 7.3 and 7.4)

We stress that when a protocol supports several hash functions, those attacks are possible as long as `SHA-1` is *supported* by implementations, even if it is not selected during normal use. A man-in-the-middle attacker will just force the parties to use `SHA-1`.

More generally, as cryptographers, we recommend to deprecate `SHA-1` everywhere, even when there is no direct evidence that this weaknesses can be exploited. `SHA-1` has been broken regarding collision resistance for 15 years, and there are better alternatives available, well-studied, and standardized (`SHA-2` [17], `SHA-3` [18]). There is no good reason to use `SHA-1` in modern security software. Attacks only get better over time, and the goal of the cryptanalysis effort is to warn users so that they can deprecate algorithms *before* the attacks get practical.

As a stopgap measure, the collision-detection library of Stevens and Shumow [26] can be used to detect attack attempts (it successfully detects our attack).

**Responsible disclosure.** We have tried to contact the authors of affected software before announcing this attack, but due to limited resources, we could not notify everyone. We detail below the main affected products, some of the responses we received, and countermeasures deployed at the time of writing. More up to date information will be available on the website of the attack: <https://sha-mbles.github.io>.

## 7.1 `SHA-1` Usage in GnuPG

There are currently two supported branches of GnuPG: GnuPGv1 is the “legacy” (or “classic”) branch, and GnuPGv2 is the “modern” branch. The first version of GnuPGv2 dates back to 2006, and the “legacy” branch is no longer recommended, but the transition took a long time. In particular, GnuPGv1 was still the default version in Fedora 29 (released in October 2018), and in Ubuntu 16.04 LTS (which is supported until April 2021).

GnuPG supports many different algorithms, including `SHA-1`. Moreover, `SHA-1` is the default algorithm for identity certification in GnuPGv1. This is why we targeted PGP in our demonstration of chosen-prefix collisions. After we disclosed our results to the GnuPG team, `SHA-1` signatures have been deprecated in the GnuPGv2 branch.

We have first discussed this attack with the GnuPG developers the 9th of May 2019 and eventually informed them of the newly found chosen-prefix collision the 1st of October 2019. The issue is tracked with CVE number CVE-2019-14855. A countermeasure has been implemented in commit `edc36f5`, included in GnuPG version 2.2.18 (released on the 25th of November 2019): `SHA-1`-based identity signatures created after 2019-01-19 are now considered invalid.

**Web of Trust.** The original trust model of PGP was the Web of Trust. Instead of using a central PKI, users sign each other’s keys to attest of their identity (*e.g.* when attending a key signing party), and trust such certificates from third parties. A scan of the PGP Web of Trust (i.e. identity certifications on public key servers) shows that roughly 1% of the identity certifications issued in 2019 use SHA-1. This probably corresponds to usage of GnuPGv1 with the default settings, and would make our attack feasible.

However the Web of Trust does not seem to be widely used anymore. In particular, after the poisoning attack at the end of June 2019 [?], GnuPG 2.2.17 and later do not import identity certificates from public key servers by default. A major usage of GnuPG is now to authenticate software packages in Linux, but this typically relies on directly trusting the relevant keys without third parties.

**CAcert.** CAcert (<http://cacert.org/>) is one of the main CAs for PGP keys, and they still use SHA-1 to sign user keys. We have first contacted them by email on December 14th, and got an answer on January 6th acknowledging this issue. They are now planning a switch to a secure hash function for key certification.

We note that our attack is not directly applicable because CAcert does not sign JPEG images in PGP keys, but using SHA-1 signature is nonetheless an important security risk.

## 7.2 SHA-1 Usage in X.509 Certificates

The CA/Browser Forum decided to sunset SHA-1 in October 2014, and its members are not supposed to issue SHA-1 certificates after 2016. Web browsers have enforced similar rules, and all modern browsers now reject SHA-1 certificates.

However, SHA-1 certificates are still present for legacy purposes, on services that are used by older clients that can not be upgraded. In particular, it remains possible to buy a SHA-1 certificate today, and there are a few recently-issued certificates in use on the web<sup>7</sup>. There are also a few old SHA-1 certificates still in use<sup>8</sup>. Those certificates are rejected by modern web browsers, but they can be accepted by non-web TLS clients. For instance, it seems that the Mail application in Windows 10 can open an IMAP session secured with a SHA-1 certificate without warning. Similarly, OpenSSL still accepts SHA-1 certificates at security level 1 (the default level in most distributions – but Debian Buster has set the default level to 2, which prevents usage of SHA-1 certificates).

Chosen-prefix collisions against MD5 have been able to break the security of certificates in the past, with the creation of a Rogue CA by Stevens *et al.*[27], and in the wild by the flame malware[21]. If some of the CAs still issuing SHA-1 certificates use predictable serial numbers, a similar attack might be possible today (being located at the beginning of the “to-be-signed” part of the certificate, if the serial number is unpredictable then the CP collision attack is thwarted as a crucial part of the hashed input is not controlled by the attacker).

## 7.3 SHA-1 Usage in TLS

Besides certificates, there are two places where SHA-1 can be used in the TLS protocol: SHA-1 can be used to sign the handshake, and HMAC-SHA-1 can be used to authenticate data in the record protocol.

<sup>7</sup>Some examples can be found by searching through certificate transparency logs: [http://web.archive.org/web/20191227165750/https://censys.io/certificates?q=tags%3Atrusted+AND+parsed.signature\\_algorithm.name%3ASHA1%2A+AND+parsed.validity.start%3A%5B2019-01-01+T0+%2A%5D](http://web.archive.org/web/20191227165750/https://censys.io/certificates?q=tags%3Atrusted+AND+parsed.signature_algorithm.name%3ASHA1%2A+AND+parsed.validity.start%3A%5B2019-01-01+T0+%2A%5D)

<sup>8</sup>As seen in this scan: [http://web.archive.org/web/20191227165038/https://censys.io/ipv4?q=443.https.tls.validation.browser\\_trusted%3AYes+AND+443.https.tls.certificate.parsed.signature\\_algorithm.name%3ASHA1%2A](http://web.archive.org/web/20191227165038/https://censys.io/ipv4?q=443.https.tls.validation.browser_trusted%3AYes+AND+443.https.tls.certificate.parsed.signature_algorithm.name%3ASHA1%2A)

**Handshake.** In order to authenticate the TLS handshake, the client and the server sign a copy of the transcript at the end of the handshake. If the hash function used in the signature is weak, an attacker can use chosen-prefix collisions to mount a man-in-the-middle attack and break various properties of the handshake, as shown by the SLOTH attacks [1]. However, this remains far from being a practical attack, because the CP collision has to be computed in a very short time frame, while the session is being established (timeout value is generally set to a few seconds, but can be up to several minutes).

In TLS 1.0 and 1.1, the handshake is hashed with the concatenation of SHA-1 and MD5. Using the multicollision attack from Joux [9], computing a CP collision for MD5 || SHA-1 is not much harder than for SHA-1. We give concrete figures in Table 2, showing that this is probably within reach of a well motivated adversary.

In TLS version 1.2, the hash function used is configurable, and is negotiated between the client and the server. MD5 was one of the possible options, but support has been removed after the SLOTH attack. However, SHA-1 is still widely supported, and many servers actually *prefer* to use SHA-1, even when the client offers better algorithms. Scan results of the top 1M websites show that 3% of them use SHA-1<sup>9</sup>, and this includes many high profile websites.<sup>10</sup> The vast majority of TLS 1.0/1.1 clients offer SHA-1 as an option for the signature.

In TLS version 1.3, MD5 and SHA-1 have been removed.

**Ciphersuites.** The ciphersuite used in a TLS connection is the result of a negotiation between the client and server, so it is hard to predict exactly. However, the large majority of clients and servers support ciphersuites where HMAC-SHA-1 is used to authenticate the packets, at least for interoperability reasons. It seems that usage of HMAC-SHA-1 represents a few percent of all the connections. Telemetry results from Mozilla report about 2% of connections with a HMAC-SHA-1 ciphersuite.<sup>11</sup> In addition, a scan of websites in the Alexa top 1M show that 8% of them would use a HMAC-SHA-1 ciphersuite with the client settings used for the scan<sup>12</sup>.

This usage is not threatened by our attack, but we recommend to avoid SHA-1 usage when possible.

**OpenSSL.** We have first contacted the OpenSSL developers on December 14th. The next version of OpenSSL will no longer allow X.509 certificates signed using SHA-1 at security level 1 and above (commit 68436f0). Since security level 1 is the default configuration for TLS/SSL, this will prevent SHA-1 usage for certificates.

Debian Linux had previously set the default configuration to security level 2 (defined as 112-bit security) in the latest release (Debian Buster); this already prevents dangerous usage of SHA-1 (for certificates and handshake signature).

## 7.4 SHA-1 Usage in SSH

SHA-1's usage in SSH is similar to its usage in TLS. The SSH-2 protocol supports usage of SHA-1 to sign the transcript (at the end of the key exchange), and HMAC-SHA-1 to authenticate the data in the record protocol. As in the TLS case, usage of SHA-1 to sign the transcript has been shown to be potentially vulnerable to the SLOTH attack [1], but

<sup>9</sup>[http://web.archive.org/web/20191227174651/https://censys.io/domain/report?field=443.https.tls.signature.hash\\_algorithm](http://web.archive.org/web/20191227174651/https://censys.io/domain/report?field=443.https.tls.signature.hash_algorithm)

<sup>10</sup>[http://web.archive.org/web/20191227174551/https://censys.io/domain?q=443.https.tls.signature.hash\\_algorithm%3Asha1](http://web.archive.org/web/20191227174551/https://censys.io/domain?q=443.https.tls.signature.hash_algorithm%3Asha1)

<sup>11</sup>See [https://telemetry.mozilla.org/new-pipeline/dist.html#!measure=SSL\\_CIPHER\\_SUITE\\_FULL](https://telemetry.mozilla.org/new-pipeline/dist.html#!measure=SSL_CIPHER_SUITE_FULL), where buckets 5, 61 and 63 correspond to HMAC-SHA-1 ciphersuites

<sup>12</sup>[http://web.archive.org/web/20191226134753/https://censys.io/domain/report?field=443.https.tls.cipher\\_suite.name.raw](http://web.archive.org/web/20191226134753/https://censys.io/domain/report?field=443.https.tls.cipher_suite.name.raw)

this is not practical given the timing constraints (usually just a few seconds, but can be configured to a longer period of time).

Again, the choice of cryptographic algorithms depends on a negotiation between the client and server, so it is hard to know exactly what will be selected. However, scans of the IPv4 space from censys at the time of writing show that roughly 17% of servers use SHA-1 to sign the transcript<sup>13</sup>, and 9% of servers use HMAC-SHA-1 in the record protocol<sup>14</sup>. This mostly corresponds to servers running old versions of SSH daemons.

**OpenSSH.** Due to our results, since version 8.2 of OpenSSH a “future deprecation notice” is included, explaining that SHA-1 signatures will be disabled in the near-future.

## 7.5 Other Usages of SHA-1

**DNSSEC.** SHA-1 is still used in DNSSEC, with 18% of the top-level domains using SHA-1 at the time of writing<sup>15</sup>. Since DNSSEC signatures include user-supplied content, CP collisions could be used to attack the DNSSEC system.

**GIT.** GIT relies heavily on SHA-1 to identify all objects in a repository. It does not necessarily require cryptographic security from SHA-1, but there are certainly some attack scenarios where attacks on SHA-1 would matter. In particular, signed GIT commits are essentially signatures of a SHA-1 hash, so they would be sensitive to collision attacks.

The GIT developers have been working on replacing SHA-1 for a while<sup>16</sup>, and they use a collision detection library [26] to mitigate the risks of collision attacks.

**Timestamping.** Many timestamping servers apparently support SHA-1, such as: <https://sectigo.com/resources/time-stamping-server>

## 8 Conclusion and Future Works

This work shows once and for all that SHA-1 should not be used in any security protocol where some kind of collision resistance is to be expected from the hash function. Continued usage of SHA-1 for certificates or for authentication of handshake messages in TLS or SSH is dangerous, and there is a concrete risk of abuse by a well-motivated adversary. SHA-1 has been broken regarding collision resistance since 2004, but it is still used in many security systems. We strongly advise users to remove SHA-1 support to avoid downgrade attacks. We exhibited a practical chosen-prefix collision attack on SHA-1, and performed an actual CP collision computation for a reasonable cost. This cost will decrease over time and in a close future will be so cheap that any ill-intentioned person could afford it.

Our work directly impacts the security of PGP/GnuPG Web of Trust: using our CP collision attack on SHA-1, we have created two PGP keys with different UserIDs and colliding certificates. This allows an attacker to impersonate any user, as long as trusted third parties sign identity certifications with SHA-1.

We also show that gaming or mining GPUs offer a cheap and efficient way to attack symmetric cryptography primitives. In particular, it now costs less than US\$ 100k to rent GPUs and break cryptography with a security level of 64 bits (i.e. to compute  $2^{64}$  operations of symmetric cryptography).

<sup>13</sup>[http://web.archive.org/web/20191226130952/https://censys.io/ipv4/report?field=22.ssh.v2.selected.kex\\_algorithm](http://web.archive.org/web/20191226130952/https://censys.io/ipv4/report?field=22.ssh.v2.selected.kex_algorithm)

<sup>14</sup>[http://web.archive.org/web/20191226131928/https://censys.io/ipv4/report?field=22.ssh.v2.selected.client\\_to\\_server.mac](http://web.archive.org/web/20191226131928/https://censys.io/ipv4/report?field=22.ssh.v2.selected.client_to_server.mac)

<sup>15</sup><https://www.dns.cam.ac.uk/news/2020-02-14-sha-mbles.html>

<sup>16</sup><https://git-scm.com/docs/hash-function-transition/>

**Future works.** The cost of our attack is roughly four times the cost of a plain collision attack, so there is limited room for improvements in terms of complexity. The factor 4 could be slightly reduced by changing the parameters of the graph, but this is unlikely to result in an improvement of more than a factor 2. Alternatively, improvements to the near-collision search could improve simultaneously identical-prefix and chosen-prefix collision attacks.

On the other hand, we believe there is some possibility to reduce the number of blocks used in the attack without increasing the complexity much. Firstly, with a better use of the global parameters of the general chosen-prefix collision attack. By playing with the number of blocks, the allowable probabilities and the size of the graph, one could probably find a better configuration. Secondly, by not considering only the core differential trail from [23], but using other interesting ones (for example the ones already used in other previous SHA-1 attacks), we would increase the pool of available differences and in turn reduce the required number of blocks.

A natural future work would be to study other applications of practical chosen-prefix collisions on SHA-1. Different protocols would lead to different constraints for the attacker, and unfortunately SHA-1 remains used on field. What would then be the security impact of our findings on these applications? What applications could be targeted?

Finally, it remains to be studied how recent chosen-prefix collision attacks could potentially apply to other hash functions, such as RIPEMD, (reduced-round) SHA-2, or even others.

We are planning to publish code to make our claims easy to verify, but due to the strong impact of this attack, we will wait until counter-measures are more widely implemented.

## Acknowledgements

The authors are grateful to the USENIX Security 2020 reviewers and shepherd for their insightful comments that improved the quality of the paper.

The authors would like to thank Vesselin Velichkov for his help with regards to an initial analysis of neutral bits applicability on SHA-1 and Werner Koch for his comments on the applicability of our attacks on PGP. The authors would also like to thank [gpusersrental.com](https://gpusersrental.com) for their efficient service regarding the GPU cluster renting. The second author is supported by Temasek Laboratories, Singapore.

A small part of the experiments presented in this paper were carried out using the Grid'5000 testbed, supported by a scientific interest group hosted by Inria and including CNRS, RENATER and several Universities as well as other organizations (see <https://www.grid5000.fr>). Development and small scale experiments before launching the main computation were carried out on the rioc cluster from Inria.

## References

- [1] Karthikeyan Bhargavan and Gaëtan Leurent. Transcript collision attacks: Breaking authentication in TLS, IKE and SSH. In *NDSS 2016*. The Internet Society, February 2016.
- [2] Eli Biham and Rafi Chen. Near-collisions of SHA-0. In Franklin [8], pages 290–305.
- [3] Eli Biham, Rafi Chen, Antoine Joux, Patrick Carribault, Christophe Lemuet, and William Jalby. Collisions of SHA-0 and reduced SHA-1. In Ronald Cramer, editor, *EUROCRYPT 2005*, volume 3494 of *LNCS*, pages 36–57. Springer, Heidelberg, May 2005.

- 
- [4] Gilles Brassard, editor. *CRYPTO*, volume 435 of *Lecture Notes in Computer Science*. Springer, 1990.
  - [5] J. Callas, L. Donnerhacker, H. Finney, D. Shaw, and R. Thayer. *RFC 4880 - OpenPGP Message Format*. Internet Activities Board, November 2007.
  - [6] Ivan Damgård. A Design Principle for Hash Functions. In Brassard [4], pages 416–427.
  - [7] Christophe De Cannière and Christian Rechberger. Finding SHA-1 characteristics: General results and applications. In Xuejia Lai and Kefei Chen, editors, *ASIACRYPT 2006*, volume 4284 of *LNCS*, pages 1–20. Springer, Heidelberg, December 2006.
  - [8] Matthew Franklin, editor. *CRYPTO 2004*, volume 3152 of *LNCS*. Springer, Heidelberg, August 2004.
  - [9] Antoine Joux. Multicollisions in iterated hash functions. Application to cascaded constructions. In Franklin [8], pages 306–316.
  - [10] Antoine Joux and Thomas Peyrin. Hash functions and the (amplified) boomerang attack. In Alfred Menezes, editor, *CRYPTO 2007*, volume 4622 of *LNCS*, pages 244–263. Springer, Heidelberg, August 2007.
  - [11] Vlastimil Klima. Tunnels in hash functions: MD5 collisions within a minute. Cryptology ePrint Archive, Report 2006/105, 2006. <http://eprint.iacr.org/2006/105>.
  - [12] Gaëtan Leurent and Thomas Peyrin. From collisions to chosen-prefix collisions application to full SHA-1. In Yuval Ishai and Vincent Rijmen, editors, *EUROCRYPT 2019, Part III*, volume 11478 of *LNCS*, pages 527–555. Springer, Heidelberg, May 2019.
  - [13] Gaëtan Leurent and Thomas Peyrin. SHA-1 is a Shambles - First Chosen-Prefix Collision on SHA-1 and Application to the PGP Web of Trust. Cryptology ePrint Archive, Report 2020/014, 2020. <https://eprint.iacr.org/2020/014>.
  - [14] Marc Stevens. Attacks on Hash Functions and Applications. PHD Thesis, Leiden University, June 2012.
  - [15] Ralph C. Merkle. One Way Hash Functions and DES. In Brassard [4], pages 428–446.
  - [16] National Institute of Standards and Technology. FIPS 180-1: Secure Hash Standard, April 1995.
  - [17] National Institute of Standards and Technology. FIPS 180-2: Secure Hash Standard, August 2002.
  - [18] National Institute of Standards and Technology. FIPS 202: SHA-3 Standard: Permutation-Based Hash and Extendable-Output Functions, August 2015.
  - [19] Ronald L. Rivest. The MD4 message digest algorithm. In Alfred J. Menezes and Scott A. Vanstone, editors, *CRYPTO'90*, volume 537 of *LNCS*, pages 303–311. Springer, Heidelberg, August 1991.
  - [20] Ronald L. Rivest. *RFC 1321: The MD5 Message-Digest Algorithm*. Internet Activities Board, April 1992.
  - [21] Marc Stevens. Counter-cryptanalysis. In Ran Canetti and Juan A. Garay, editors, *CRYPTO 2013, Part I*, volume 8042 of *LNCS*, pages 129–146. Springer, Heidelberg, August 2013.

- 
- [22] Marc Stevens. New collision attacks on SHA-1 based on optimal joint local-collision analysis. In Thomas Johansson and Phong Q. Nguyen, editors, *EUROCRYPT 2013*, volume 7881 of *LNCS*, pages 245–261. Springer, Heidelberg, May 2013.
- [23] Marc Stevens, Elie Bursztein, Pierre Karpman, Ange Albertini, and Yarik Markov. The first collision for full SHA-1. In Jonathan Katz and Hovav Shacham, editors, *CRYPTO 2017, Part I*, volume 10401 of *LNCS*, pages 570–596. Springer, Heidelberg, August 2017.
- [24] Marc Stevens, Pierre Karpman, and Thomas Peyrin. Freestart collision for full SHA-1. In Marc Fischlin and Jean-Sébastien Coron, editors, *EUROCRYPT 2016, Part I*, volume 9665 of *LNCS*, pages 459–483. Springer, Heidelberg, May 2016.
- [25] Marc Stevens, Arjen K. Lenstra, and Benne de Weger. Chosen-prefix collisions for MD5 and colliding X.509 certificates for different identities. In Moni Naor, editor, *EUROCRYPT 2007*, volume 4515 of *LNCS*, pages 1–22. Springer, Heidelberg, May 2007.
- [26] Marc Stevens and Daniel Shumow. Speeding up detection of SHA-1 collision attacks using unavoidable attack conditions. In Engin Kirda and Thomas Ristenpart, editors, *USENIX Security 2017*, pages 881–897. USENIX Association, August 2017.
- [27] Marc Stevens, Alexander Sotirov, Jacob Appelbaum, Arjen K. Lenstra, David Molnar, Dag Arne Osvik, and Benne de Weger. Short chosen-prefix collisions for MD5 and the creation of a rogue CA certificate. In Shai Halevi, editor, *CRYPTO 2009*, volume 5677 of *LNCS*, pages 55–69. Springer, Heidelberg, August 2009.
- [28] Paul C. van Oorschot and Michael J. Wiener. Parallel collision search with cryptanalytic applications. *Journal of Cryptology*, 12(1):1–28, January 1999.
- [29] Xiaoyun Wang, Yiqun Lisa Yin, and Hongbo Yu. Finding collisions in the full SHA-1. In Victor Shoup, editor, *CRYPTO 2005*, volume 3621 of *LNCS*, pages 17–36. Springer, Heidelberg, August 2005.



## A Improving SHA-1 Collision Attack

We now give the technical details of the improvements introduced in Section 3, for readers that are familiar with previous works [22, 23, 12].

### A.1 Boomerangs and Neutral Bits

As explained in [12], an important factor to evaluate the cost of the attack is the number of boomerangs available when looking for a conforming message. The collision attack from Eurocrypt 2013 [22] and its GPU implementation from Crypto 2017 [23] (the “Shattered” attack) use three boomerangs, on bits 6 and 8 of  $M_6$  (red type in Figure 9), and on bit 7 of  $M_9$  (blue type in Figure 9). However, the boomerang on  $M_6[8]$  actually flips the value of  $W_{77}[0]$  due to the message expansion, and breaks the condition  $W_{77}[0] \oplus W_{77}[2] = 1$  listed on Table 5 of [23]. This reduces the probability of the trail on rounds 61–80 by a factor  $3/4$ , from  $2^{-19.17}$  to  $2^{-19.58}$ . However, the boomerang almost doubles the number of partial solution produced, so that using it still improves the attack.

In addition, we realized that the “Shattered” attack [23] uses a neutral bit on  $M_{13}[11]$ . However, this breaks the condition  $W_{76}[0] \oplus W_{76}[1] = 1$ , and reduces the probability of the trail by a factor roughly  $2^{0.2}$ . In our analysis, we assume that this neutral bit has been removed: since it has a very small effect on the number of partial solution produced, it reduces the complexity of the attack by a factor  $2^{0.2}$ . In particular, this is why we consider that a collision requires  $2^{48.5}$   $A_{33}$ -solutions rather than  $2^{48.7}$  (where an  $A_i$ -solution refers to an input pair that is following the differential path until word  $A_i$  inclusive).

In our chosen-prefix attack, we also need conditions on  $W_{77}[0]$ , and we decided to remove the boomerang on  $M_6[8]$  in order to keep more control on the output difference and to simplify the attack. In particular, removing this boomerang makes easier the construction of trails with the extra constraints (and we have successfully built trails with the two remaining boomerangs for all successive blocks). This implies that the cost of near-collision blocks increases by a factor  $3/2$  compared to the “Shattered” attack, leading to  $C_{\text{block}} = 2^{64.9}$  on a GTX 970 (after gaining a factor  $2^{0.2}$  by removing  $M_{13}[11]$  as a neutral bit). Therefore we can estimate more accurately the complexity of the previous attack [12] as  $2^{67.1}$  SHA-1 computations, instead of the range of  $2^{66.9}$  to  $2^{69.4}$  reported previously (the optimal attack parameter choice for [12] is then a maximum cost of  $3.5 C_{\text{block}}$ ).

As an optimization, we decided to use the boomerang on  $M_6[8]$  for the last block, because the computation of the last block is identical to the second block of an identical-prefix collision attack. In particular, we had no trouble building a path with this boomerang, and this results in a speed-up of a factor 1.9 in the rate of  $A_{33}$ -solutions. We need to increase the number of solutions by a factor  $4/3$  because the solutions are of lower quality, but this still corresponds to a speed-up factor of roughly 1.4. Since the last block represents a significant part of the total computation, this is a worthwhile optimization.

### A.2 Additional Boomerangs and Modular Correction

We found out that in addition to previously mentioned boomerangs, we can use very short boomerangs on bits 4, 5, and 6 of  $M_{11}$  (green type in Figure 9), with a single correction on  $M_{12}$ . These boomerangs are neutral until step 22, like the boomerang on  $M_9$ . The problem is that they will clash with existing small boomerangs starting at  $M_6[6]$ ,  $M_6[8]$  and  $M_9[7]$ .

More precisely, the boomerang starting at  $M_{11}[4]$  will flip the message condition “ $\bar{x}$ ” from the boomerang starting at  $M_6[6]$ , corresponding to the last message correction of the local collision. In order to avoid this issue, we simply change the last correction of the  $M_6[6]$  boomerang to be a modular addition correction instead of an XOR correction. This

$i$	$A_i$	$W_i$
-1:	-----	-----
00:	-----	-----
01:	-----	-----
02:	-----	-----
03:	-----	-----
04:	-----	-----
05:	-----	-----
06:	-----	-----x
07:	-----x	-----x̄
08:	----- 0	-----
09:	----- 1	-----y
10:	----- y	-----ȳ
11:	----- 0	-----z
12:	-----z-1	-----z̄
13:	-----0	-----
14:	-----1	-----ȳ
15:	-----	-----

**Figure 9:** Boomerangs’ differential paths used for SHA-1 with the corresponding constraints forced in order to have probability one in the 16 first steps. The red one (perturbation  $x$ ) represents a small boomerang (named  $AP_1$  in [?]) composed of a single local collision starting on  $M_6$ , here positioned at bit  $j = 2$ . The blue one (perturbation  $y$ ) represents another small boomerang used in [22, 23], also composed of a single local collision, but starting on  $M_9$ , here positioned at bit  $j = 14$ . The green one (perturbation  $z$ ) represents a new and even smaller boomerang built from a partial local collision starting on  $M_{11}$ , here positioned at bit  $j = 25$ . The MSB’s are on the right and “-” stands for no constraint. The letters represent a bit value and its complement is denoted by an upper bar on the corresponding letter. The notation “|” on two bits vertically adjacent mean that these two bits must be equal.

$i$	$A_i$	$W_i$
-1:	-----	-----
00:	-----	-----
01:	-----	-----
02:	-----	-----
03:	-----	-----
04:	-----	-----
05:	-----	-----
06:	-----	-----0-0
07:	-----0-0	-----1-1
08:	----- 0-0	-----
09:	----- 1-1	-----0
10:	----- 0	-----1
11:	----- 00	-----111
12:	-----111	-----
13:	-----000	-----1
14:	-----111	-----1
15:	-----	-----

**Figure 10:** Exact conditions required to prepare all the boomerangs’ differential paths used for our CP collision attack on SHA-1 with the corresponding constraints forced in order to have probability one in the 16 first steps. The MSB’s are on the right and “-” stands for no constraint. The notation “|” on two bits vertically adjacent mean that these two bits must be equal. These conditions basically correspond to very short boomerangs started at  $M_{11}[4]$ ,  $M_{11}[5]$  and  $M_{11}[6]$ , and small boomerangs started at  $M_6[6]$ ,  $M_6[8]$  and  $M_9[7]$  (boomerang starting perturbations are marked in purple). We remark an extra condition  $M_{13}[5] = 1$  in order to potentially correct the clash between boomerangs  $M_{11}[5]$  and  $M_9[7]$ .

will naturally correct the perturbation as the step operation involved is indeed a modular addition and the boomerang on  $M_6[6]$  will behave as expected (the condition “ $\bar{x}$ ” is actually not needed anymore). This can be seen as a generalization of the boomerang strategy used so far for SHA-1: boomerang corrections can be applied modular addition-wise instead of XOR-wise. This will induce changes in subsequent bits in the corresponding message words because of carry propagations that might naturally occur with a modular addition operation, but as long as these bit changes do not mess with existing message conditions, we are fine<sup>17</sup>. This idea might also be interesting to analyse other hash functions.

Similarly, the boomerang starting at  $M_{11}[6]$  will flip the message condition “ $\bar{x}$ ” from the boomerang starting at  $M_6[8]$ , corresponding to the last message correction of the local collision. This is exactly the same situation and we avoid this issue by changing the last correction of the  $M_6[8]$  boomerang to be a modular addition correction instead of an XOR correction.

Finally, the boomerang starting at  $M_{11}[5]$  will flip the condition “1” in the internal state, required for the boomerang starting at  $M_9[7]$ . This will create an uncontrolled difference when we use the  $M_9[7]$  boomerang, that we correct by introducing a new difference in  $M_{13}[5]$  (setting the extra condition  $M_{13}[5] = M_9[7] \oplus 1$  will ensure a proper correction using XOR correction). Note that we perform this further correction only in the case where the boomerang starting at  $M_{11}[5]$  was triggered. We observe furthermore that the correction on  $M_{13}[5]$  will maintain a good quality of neutrality for  $M_{11}[5]$  boomerang. All the conditions required to use the boomerangs are given in Figure 10.

---

<sup>17</sup>In more details, since the boomerangs on  $M_{11}[4]$ ,  $M_{11}[5]$  and  $M_{11}[6]$  are very short and thus applied before boomerangs  $M_6[6]$ ,  $M_6[8]$  and  $M_9[7]$ , we don't actually care if the last ones break conditions of the first ones since they have already been used.

# B Chosen-prefix Collision Example

```

-----BEGIN PGP PUBLIC KEY BLOCK-----

mQNBH/0F4ABGAD/UHJhY3RpY2FsIFNlQ3R0eXNlbnNlbnVmaXgY29sbGZl
aW9uR0R0bGUmYEEEdh99dn8HYkndx/szLU4wrDXb7Hnqsr4WdLfbDeLTLcy/h
1R20CYHcqUQf0H26Au5130tjGhSSk+dX83tzQesn0GSMa86KwDU1Df2y1Nlnhy
n+5VMxm23Mxhn8pPuTtW7HLeMKCH6jrmc1mi7iCyDXKxtk/syQhPw8yzzd7Yt16
KEMGFqr/bCZY+n+Uj4ihBe95v7E7NeU00S19XLB67008R9uALwBDQHPcTeK0+ZBmX
3I6NDTP4nyTEb+Hqun81tMf7gnK2xQ7auot811W7LC/FAljn5VwzaLENT/9X6/j
z8rAmBJsZxHoJxBeReOqkOCWjQaKs+13mT0evncwbVnqfeyWdW81Y9xa/OwkyT
LKprFBin9U8wS0aToUyZ1i/ZjYrUJ23q1vFNtGcvIy9GhZCLZ19YmtPwgJzQ
K/34boJfxHcNDAPcRU0Xcst56E98uk31FNvz22j78Cp6d0yuaFtpv0WNAQphv
xHv7uGvImR/Ca1PyaumGpGT77MozQs1D4JrzE1JULGXTJ1PwCYbo8f/AG1Hf
FOa/xhubrubB1KrpNvdKAMOPbpcFtQdQSKTm/WSj5jC2TY+Pv1881Ncvyj1a473
01Z25IXMqPTX3QcmXkE9Wew05xwGhX7b20es/U15qoGmrot/vF84gWkBPdJEvxV
QUH925zyRyBQoQfEKmD8s8mQG/38eDGSUA6+OzYycsz5XBzSNIeF2VYm40nZjBR
g4/DsgPgmw2c09229GQHQYH9nQNL0ASAgwRjx1Z1J1+xnAC1ehPvIm1PrsY1Es
1ZJZuZjfmFR1VUB8DRXshFngA85n1vVont7fAnZTYnyM5PM5ZBHTH/91uEwef+
vMgBv5t3S1T2m6dEqgStX1k3kNZ77jy93AD0e64i5vmCSTUNoSgz7A0+6KzQ21R
+zb0/Aku29MeHnCAEQEAABQVQm91Dxi02JAZXhnbXBSZ55j20+1QUUBMBCAA+
F1EExr/1/Lv1Gokr63EYjPuzGH2cQqFAn/of4AC0G8FCQABUYAFOWk1Bw1GFQqJ
CAsCBYCAwEChgECP4AAcGkEjPUzGh2cSLZhgAynF426x93af2jzWUFWMZ
duiZ78Jwpp0Gn/BrAs1D/dmmK/UjAVfG7aCq/R/Fd3faeA1qxJSt6Z2bDcbtJ
HjERNPaTeKJaHP4EgHsFSD2QUMdUwS07rc1XmHm7AxCKfXg+USR1cxQkyB1L7
U9uXleM06+Fr+QP2y4MsZpM1n1pJk1FuKkQeY17Rdr0Ljyq1Vf0Tq16kr2
tzk10Q2Cs+Rmi4dC0MMAa1L5tppm1PMo3YqV01Crqeyf0YUPLI29DHBMDf1z
213eWgUpHhBvERS0rwxv/4eizUgmisgjrWjhdhGhZfWmZQVfvtzjz7WwhVpV
va5+286YayrD81j1w7fFKF4PH1t11awCwGsei89EAcYF4MzGw/1YjQWlhBvV
e+NeKRSjI5o3ZS8bQvD1/DgJ4Go9J3KXXKjSbaxedakSS44XU054AnG7j10ak5
YHkDrjZYdtE1zkKj1UEYdYqA51cRjJ2Kiy3g4x1R+7ev611Q80au8Y1q6Q7me0
451KG17m0e6qMPrP95Tuae/VfjZaysR4nUX1Z11k6sfgZQ7F1ohY0SSfYvFrj
dtpG01XeKXnEkaub929C0U1h6SRL7/xk968Kq17SoMIMFspMuskfAn/e6ipbn
u2c0jPThnELZjmvh0Kct/x6jv1vbdU1B+gg25BTDqFm0ir20XFK1Rz6PuhG14
dQKbSmbJtUgTDEogR1HUZ2CXWpJ5z89xvcGvaTPurqnc0Ez668K5Y1PSPDw0x
tIxEaupvGnug4/Ct1vFE+vF7ZcMSThLLXJVRATNcWosfXmW44ALebbxqZ1
ukwJmJ0et85Zhb1FRm3MgHP7hjqJqE5XovZLqLKRr3dqZ7hmX0j0eAT0II
Bkvv1Jh8XU293h8v8H4wGRVPvyHrTiWcWj+pgb4YTPShoys0NIE9543cy1c94+
s1ak45aakyHC90Rw0raF0yED19ewSf15N3zW1XiJc2B8AGAGBQJ/6VrWA0J
EK+7H+1pUa116U8/3HGCKMjYdRr181ZrMwCf0x11C1k156K2ZV8sg/RL2c0
GJzr0p3+fgQjRfMnE+5Sc1Ih3L3PgsCTEO0Cma3+jo7s8fnhLzVzhjCJEXp
fo4z1r9Kh5cUXLSzR2XCHE/11dEXjE1e6fS9a5hndVnB4wC0nCRHY/t1bn
tW1a3m8w9zrTCDVxHNSj6mS01y+1J1U3I6H+Pj0X6YyMeDwvW0Cn/q1tm7U
K2YwV82cKqVqYIPG5mGQC21sDmTP3ct+VMrJD48+S2EmorInhmKruT5b5
7p6AHUExh1P1TSRvGpGjnzDGuP6TUBVUGRE7MvFnW4V0EABEAAAAAAAAAAAA
AAAA/9j/2wDAP//////////AALCABAAPgBARA/8QAAABAQEA
AAAAAAAAAAAAAAAAAEEAEEAAAAAAAAAAAAAAAAAAAAAA/9oACAEBA/ANB0AE6
gATqTqAB0AA0E0KE4KE4oTgAAoTgAKE4oTqAB0oTqAT1h0KA/2V24m85L1zd
vR0CAo21Z1yb/Mh+1zms0zsu52BkJUC+e/UPmKQ4S0M8E0A0EQA0EQA0AAZ
QWxpY2UgPGFsaW11Gv4Yw1vWGUy29PoxdVAGTA0gAPYHMA/4vY75RqJK+3
mE1z1Mx29nEBQJ/6B44AhsVbQkAAVGAQBsJCAcCBUyK0GfLAgQWAgB4h4BAhE
AAcJEB1z1Mx29nEBnK1ALms73X14/+0sUPj0jwYUe6F8Y67/1h0b25Bclp3qoz
4ESkF1g2ZuAEbMs31ANy7zvZpZrgYdSEBAbsuP8MxerGow0a3Clas5wP9ooh
0wgh10vTuz2G6odJhN0RnZ/BW1az1Y0Zaz1i0QZm+67BfURJ10fHgND0OZ2KE
f2ncC3vmyh9/8QhUF553KdX08VYNN0/S/GS8MD1eP4YpA3zDmZahyTzFm1
14apEERudob/PSn98dHDjQ2Wq0bE11L1VnAN1i0P+8STVbCREJm72V1j
ADP5nK3HPKegRnRuk2VtdQkyT3UBechngK+u7x1Z4G6Q9B2H/c23abxFz
vr1cBcQnqrTznUdIaxG8nmuAbk6M65M0z0eTIdct0bR7Mq84C6Vsptho3k
5dSoms1ni0L11EFTS1YUJW0V7+8UvzrAKg98buaAH1n8p8eM8bms0B016h
rJ0EfhgYB6c60hLahjPbh5Hxngy1u1ZrctK+eW0YyZRA6/pZNS7E4D
1z01S68p5yBHB5t242ytrZbVpGEx0ka47YEMKqB0+m8V3k1sk6+kbaK2cJy
A11819T48a9e0dWm+rPkZ25b1+dwQ6GS2B4d4EfqERdIgp97dJa23y7
ORR+Kt9p0JHD11UBda3M8PeYh1M0WwUw1SuB5+/fsL1NngY7Tgqv4F3Kmg/
3Zc1gmKRG7VY3D17PLZJmSvpuGdy2pqa0c+n1j0w67qUm80HbWwhh
xZkFbD6V/7iW1ChPdm1teKW/pXBAJh9A9h8T3BR1T00S25a2a6EYF5W+wh
/rh11c6SE6SEar+f+crz4Kak4HDQ4pYJ11WgWb2+e2qYH4i3KArmmfJU
3naa7LDLUKE57U2tPyg1Zf7C529sR0q50J1agcah8J1426Gw4aBQML69uU
60uHmZCPy+1S3Fjp19/YkBAHQAOA1BgUCF+1a8AAKRCvux/tvCPWZ9B/uJ
goGtG011280puoSLP811EzUDDQCPW1LLd/15JRS1m+u8YmV1LHLL1m+13463Q
6VU/Ck7089v3v0NCHAQ0U24GQ883N1Rr1CMK6/MT1YK1V1p+rADG7k1TNEpd/
13ixZfYR2ab7L7CthJoKxdior76MSRXYfMK9J1eXRM6G7jcd/E8tCkYAvEqY
yHDKqzS085EjZzrBBKLnRuessfBy2W1U1q4rTXWv4d8WcYXqB21UMjZ
w4fAKM+XgkEMOA/Gg75
=T/D4
-----END PGP PUBLIC KEY BLOCK-----

```

Figure 11: Key A

```

-----BEGIN PGP PUBLIC KEY BLOCK-----

mQNBH/0F4ABGAD/UHJhY3RpY2FsIFNlQ3R0eXNlbnNlbnVmaXgY29sbGZl
aW9uR0R0bGUmYEEEdh99dn8HYkndx/szLU4wrDXb7Hnqsr4WdLfbDeLTLcy/h
1R20CYHcqUQf0H26Au5130tjGhSSk+dX83tzQesn0GSMa86KwDU1Df2y1Nlnhy
n+5VMxm23Mxhn8pPuTtW7HLeMKCH6jrmc1mi7iCyDXKxtk/syQhPw8yzzd7Yt16
KEMGFqr/bCZY+n+Uj4ihBe95v7E7NeU00S19XLB67008R9uALwBDQHPcTeK0+ZBmX
3I6NDTP4nyTEb+Hqun81tMf7gnK2xQ7auot811W7LC/FAljn5VwzaLENT/9X6/j
z8rAmBJsZxHoJxBeReOqkOCWjQaKs+13mT0evncwbVnqfeyWdW81Y9xa/OwkyT
LKprFBin9U8wS0aToUyZ1i/ZjYrUJ23q1vFNtGcvIy9GhZCLZ19YmtPwgJzQ
K/34boJfxHcNDAPcRU0Xcst56E98uk31FNvz22j78Cp6d0yuaFtpv0WNAQphv
xHv7uGvImR/Ca1PyaumGpGT77MozQs1D4JrzE1JULGXTJ1PwCYbo8f/AG1Hf
FOa/xhubrubB1KrpNvdKAMOPbpcFtQdQSKTm/WSj5jC2TY+Pv1881Ncvyj1a473
01Z25IXMqPTX3QcmXkE9Wew05xwGhX7b20es/U15qoGmrot/vF84gWkBPdJEvxV
QUH925zyRyBQoQfEKmD8s8mQG/38eDGSUA6+OzYycsz5XBzSNIeF2VYm40nZjBR
g4/DsgPgmw2c09229GQHQYH9nQNL0ASAgwRjx1Z1J1+xnAC1ehPvIm1PrsY1Es
1ZJZuZjfmFR1VUB8DRXshFngA85n1vVont7fAnZTYnyM5PM5ZBHTH/91uEwef+
vMgBv5t3S1T2m6dEqgStX1k3kNZ77jy93AD0e64i5vmCSTUNoSgz7A0+6KzQ21R
+zb0/Aku29MeHnCAEQEAABQVQm91Dxi02JAZXhnbXBSZ55j20+1QUUBMBCAA+
F1EExr/1/Lv1Gokr63EYjPuzGH2cQqFAn/of4AC0G8FCQABUYAFOWk1Bw1GFQqJ
CAsCBYCAwEChgECP4AAcGkEjPUzGh2cSLZhgAynF426x93af2jzWUFWMZ
duiZ78Jwpp0Gn/BrAs1D/dmmK/UjAVfG7aCq/R/Fd3faeA1qxJSt6Z2bDcbtJ
HjERNPaTeKJaHP4EgHsFSD2QUMdUwS07rc1XmHm7AxCKfXg+USR1cxQkyB1L7
U9uXleM06+Fr+QP2y4MsZpM1n1pJk1FuKkQeY17Rdr0Ljyq1Vf0Tq16kr2
tzk10Q2Cs+Rmi4dC0MMAa1L5tppm1PMo3YqV01Crqeyf0YUPLI29DHBMDf1z
213eWgUpHhBvERS0rwxv/4eizUgmisgjrWjhdhGhZfWmZQVfvtzjz7WwhVpV
va5+286YayrD81j1w7fFKF4PH1t11awCwGsei89EAcYF4MzGw/1YjQWlhBvV
e+NeKRSjI5o3ZS8bQvD1/DgJ4Go9J3KXXKjSbaxedakSS44XU054AnG7j10ak5
YHkDrjZYdtE1zkKj1UEYdYqA51cRjJ2Kiy3g4x1R+7ev611Q80au8Y1q6Q7me0
451KG17m0e6qMPrP95Tuae/VfjZaysR4nUX1Z11k6sfgZQ7F1ohY0SSfYvFrj
dtpG01XeKXnEkaub929C0U1h6SRL7/xk968Kq17SoMIMFspMuskfAn/e6ipbn
u2c0jPThnELZjmvh0Kct/x6jv1vbdU1B+gg25BTDqFm0ir20XFK1Rz6PuhG14
dQKbSmbJtUgTDEogR1HUZ2CXWpJ5z89xvcGvaTPurqnc0Ez668K5Y1PSPDw0x
tIxEaupvGnug4/Ct1vFE+vF7ZcMSThLLXJVRATNcWosfXmW44ALebbxqZ1
ukwJmJ0et85Zhb1FRm3MgHP7hjqJqE5XovZLqLKRr3dqZ7hmX0j0eAT0II
Bkvv1Jh8XU293h8v8H4wGRVPvyHrTiWcWj+pgb4YTPShoys0NIE9543cy1c94+
s1ak45aakyHC90Rw0raF0yED19ewSf15N3zW1XiJc2B8AGAGBQJ/6VrWA0J
EK+7H+1pUa116U8/3HGCKMjYdRr181ZrMwCf0x11C1k156K2ZV8sg/RL2c0
GJzr0p3+fgQjRfMnE+5Sc1Ih3L3PgsCTEO0Cma3+jo7s8fnhLzVzhjCJEXp
fo4z1r9Kh5cUXLSzR2XCHE/11dEXjE1e6fS9a5hndVnB4wC0nCRHY/t1bn
tW1a3m8w9zrTCDVxHNSj6mS01y+1J1U3I6H+Pj0X6YyMeDwvW0Cn/q1tm7U
K2YwV82cKqVqYIPG5mGQC21sDmTP3ct+VMrJD48+S2EmorInhmKruT5b5
7p6AHUExh1P1TSRvGpGjnzDGuP6TUBVUGRE7MvFnW4V0EABEAAAAAAAAAAAA
AAAA/9j/2wDAP//////////AALCABAAPgBARA/8QAAABAQEA
AAAAAAAAAAAAAAAAAEEAEEAAAAAAAAAAAAAAAAAAAAAA/9oACAEBA/ANB0AE6
gATqTqAB0AA0E0KE4KE4oTgAAoTgAKE4oTqAB0oTqAT1h0KA/2V24m85L1zd
vR0CAo21Z1yb/Mh+1zms0zsu52BkJUC+e/UPmKQ4S0M8E0A0EQA0EQA0AAZ
QWxpY2UgPGFsaW11Gv4Yw1vWGUy29PoxdVAGTA0gAPYHMA/4vY75RqJK+3
mE1z1Mx29nEBQJ/6B44AhsVbQkAAVGAQBsJCAcCBUyK0GfLAgQWAgB4h4BAhE
AAcJEB1z1Mx29nEBnK1ALms73X14/+0sUPj0jwYUe6F8Y67/1h0b25Bclp3qoz
4ESkF1g2ZuAEbMs31ANy7zvZpZrgYdSEBAbsuP8MxerGow0a3Clas5wP9ooh
0wgh10vTuz2G6odJhN0RnZ/BW1az1Y0Zaz1i0QZm+67BfURJ10fHgND0OZ2KE
f2ncC3vmyh9/8QhUF553KdX08VYNN0/S/GS8MD1eP4YpA3zDmZahyTzFm1
14apEERudob/PSn98dHDjQ2Wq0bE11L1VnAN1i0P+8STVbCREJm72V1j
ADP5nK3HPKegRnRuk2VtdQkyT3UBechngK+u7x1Z4G6Q9B2H/c23abxFz
vr1cBcQnqrTznUdIaxG8nmuAbk6M65M0z0eTIdct0bR7Mq84C6Vsptho3k
5dSoms1ni0L11EFTS1YUJW0V7+8UvzrAKg98buaAH1n8p8eM8bms0B016h
rJ0EfhgYB6c60hLahjPbh5Hxngy1u1ZrctK+eW0YyZRA6/pZNS7E4D
1z01S68p5yBHB5t242ytrZbVpGEx0ka47YEMKqB0+m8V3k1sk6+kbaK2cJy
A11819T48a9e0dWm+rPkZ25b1+dwQ6GS2B4d4EfqERdIgp97dJa23y7
ORR+Kt9p0JHD11UBda3M8PeYh1M0WwUw1SuB5+/fsL1NngY7Tgqv4F3Kmg/
3Zc1gmKRG7VY3D17PLZJmSvpuGdy2pqa0c+n1j0w67qUm80HbWwhh
xZkFbD6V/7iW1ChPdm1teKW/pXBAJh9A9h8T3BR1T00S25a2a6EYF5W+wh
/rh11c6SE6SEar+f+crz4Kak4HDQ4pYJ11WgWb2+e2qYH4i3KArmmfJU
3naa7LDLUKE57U2tPyg1Zf7C529sR0q50J1agcah8J1426Gw4aBQML69uU
60uHmZCPy+1S3Fjp19/YkBAHQAOA1BgUCF+1a8AAKRCvux/tvCPWZ9B/uJ
goGtG011280puoSLP811EzUDDQCPW1LLd/15JRS1m+u8YmV1LHLL1m+13463Q
6VU/Ck7089v3v0NCHAQ0U24GQ883N1Rr1CMK6/MT1YK1V1p+rADG7k1TNEpd/
13ixZfYR2ab7L7CthJoKxdior76MSRXYfMK9J1eXRM6G7jcd/E8tCkYAvEqY
yHDKqzS085EjZzrBBKLnRuessfBy2W1U1q4rTXWv4d8WcYXqB21UMjZ
w4fAKM+XgkEMOA/Gg75
=T/D4
-----END PGP PUBLIC KEY BLOCK-----

```

Figure 12: Key B

	Message A	Message B
0x0000	99 04 0d 04 7f e8 17 80 01 20 00 ff 4b 65 79 20 69 73 20 70 61 72 74 20 6f 66 20 61 20 63 6f 6c 6c 69 73 69 6f 6e 21 20 49 74 27 73 20 61 20 74 72 61 70 21 79 c6 1a f0 af cc 05 45 15 d9 27 4e	99 03 0d 04 7f e8 17 80 01 18 00 ff 50 72 61 63 74 69 63 61 6c 20 53 48 41 2d 31 20 63 68 6f 73 65 6e 2d 70 72 65 66 69 78 20 63 6f 6c 6c 69 73 69 6f 6e 21 1d 27 6c 6b a6 61 e1 04 0e 1f 7d 76
0x0040	73 07 62 4b 1d c7 fb 23 98 8b b8 de 8b 57 5d ba 7b 9e ab 31 c1 67 4b 6d 97 43 78 a8 27 73 2f f5 85 1c 76 a2 e6 07 72 b5 a4 7c e1 ea c4 0b b9 93 c1 2d 8c 70 e2 4a 4f 8d 5f cd ed c1 b3 2c 9c f1	7f 07 62 49 dd c7 fb 33 2c 8b b8 c2 b7 57 5d be c7 9e ab 2b e1 67 4b 7d b3 43 78 b4 cb 73 2f e1 89 1c 76 a0 26 07 72 a5 10 7c e1 f6 e8 0b b9 97 7d 2d 8c 68 52 4a 4f 9d 5f cd ed cd 0b 2c 9c e1
0x0080	9e 31 af 24 29 75 9d 42 e4 df db 31 71 9f 58 76 23 ee 55 29 39 b6 dc dc 45 9f ca 53 55 3b 70 f8 7e de 30 a2 47 ea 3a f6 c7 59 a2 f2 0b 32 0d 76 0d b6 4f f4 79 08 4f d3 cc b3 cd d4 83 62 d9 6a	92 31 af 26 e9 75 9d 52 50 df db 2d 4d 9f 58 72 9f ee 55 33 19 b6 dc cc 61 9f ca 4f b9 3b 70 ec 72 de 30 a0 87 ea 3a e6 73 59 a2 ee 27 32 0d 72 b1 b6 4f ec c9 08 4f c3 cc b3 cd d8 3b 62 d9 7a
0x00c0	9c 43 06 17 ca ff 6c 36 c6 37 e5 3f de 28 41 7f 62 6f ec 54 ed 79 43 a4 6e 5f 57 30 f2 bb 38 fb 1d f6 e0 09 00 10 d0 0e 24 ad 78 bf 92 64 19 93 60 8e 8d 15 8a 78 9f 34 c4 6f e1 e6 02 7f 35 a4	90 43 06 15 0a ff 6c 26 72 37 e5 23 e2 28 41 7b de 6f ec 4e cd 79 43 b4 4a 5f 57 2c 1e bb 38 ef 11 f6 e0 0b c0 10 d0 1e 90 ad 78 a3 be 64 19 97 dc 8e 8d 0d 3a 78 9f 24 c4 6f e1 ea ba 7f 35 b4
0x0100	cb fb 82 70 76 c5 0e ca 0e 8b 7c ca 69 bb 2c 2b 79 02 59 f9 bf 95 70 dd 8d 44 37 a3 11 5f af f7 c3 ca c0 9a d2 52 66 05 5c 27 10 47 55 17 8e ae ff 82 5a 2c aa 2a cf b5 de 64 ce 76 41 dc 59 a5	c7 fb 82 72 b6 c5 0e da ba 8b 7c d6 55 bb 2c 2f c5 02 59 e3 9f 95 70 cd a9 44 37 bf fd 5f af e3 cf ca c0 98 12 52 66 15 e8 27 10 5b 79 17 8e aa 43 82 5a 34 1a 2a cf a5 de 64 ce 7a f9 dc 59 b5
0x0140	41 a9 fc 9c 75 67 56 e2 e2 3d c7 13 c8 c2 4c 97 90 aa 6b 0e 38 a7 f5 5f 14 45 2a 1c a2 85 0d dd 95 62 fd 9a 18 ad 42 49 6a a9 70 08 f7 46 72 f6 8e f4 61 eb 88 b0 99 33 d6 26 b4 f9 18 74 9c c0	4d a9 fc 9e b5 67 56 f2 56 3d c7 0f f4 c2 4c 93 2c aa 6b 14 18 a7 f5 4f 30 45 2a 00 4e 85 0d c9 99 62 fd 98 d8 ad 42 59 de a9 70 14 db 46 72 f2 32 f4 61 f3 38 b0 99 23 d6 26 b4 f5 a0 74 9c d0
0x0180	27 fd dd 6c 42 5f c4 21 68 35 d0 13 4d 15 28 5b ab 2c b7 84 a4 f7 cb b4 fb 51 4d 4b f0 f6 23 7c f0 0a 9e 9f 13 2b 9a 06 6e 6f d1 7f 6c 42 98 74 78 58 6f f6 51 af 96 74 7f b4 26 b9 87 2b 9a 88	2b fd dd 6e 82 5f c4 31 dc 35 d0 0f 71 15 28 5f 17 2c b7 9e 84 f7 cb a4 df 51 4d 57 1c f6 23 68 fc 0a 9e 9d d3 2b 9a 16 da 6f d1 63 40 42 98 70 c4 58 6f ee e1 af 96 64 7f b4 26 b5 3f 2b 9a 98
0x01c0	e4 06 3f 59 bb 33 4c c0 06 50 f8 3a 80 c4 27 51 b7 19 74 d3 00 fc 28 19 a2 e8 f1 e3 2c 1b 51 cb 18 e6 bf c4 db 9b ae f6 75 d4 aa f5 b1 57 4a 04 7f 8f 6d d2 ec 15 3a 93 41 22 93 97 4d 92 8f 88	e8 06 3f 5b 7b 33 4c d0 b2 50 f8 26 bc c4 27 55 0b 19 74 c9 20 fc 28 09 86 e8 f1 ff c0 1b 51 df 14 e6 bf c6 1b 9b ae e6 c1 d4 aa e9 9d 57 4a 00 c3 8f 6d ca 5c 15 3a 83 41 22 93 9b f5 92 8f 98
0x0200	ce d9 36 3c fe f9 7c e2 e7 42 bf 34 c9 6b 8e f3 87 56 76 fe a5 cc a8 e5 f7 de a0 ba b2 41 3d 4d e0 0e e7 1e e0 1f 16 2b db 6d 1e af d9 25 e6 ae ba ae 6a 35 4e f1 7c f2 05 a4 04 fb db 12 fc 45	c2 d9 36 3e 3e f9 7c f2 53 42 bf 28 f5 6b 8e f7 3b 56 76 e4 85 cc a8 f5 d3 de a0 a6 5e 41 3d 59 ec 0e e7 1c 20 1f 16 3b 6f 6d 1e b3 f5 25 e6 aa 06 ae 6a 2d fe f1 7c e2 05 a4 04 f7 63 12 fc 55
0x0240	4d 41 fd d9 5c f2 45 96 64 a2 ad 03 2d 1d a6 0a 73 26 40 75 d7 f1 e0 d6 c1 40 3a e7 a0 d8 61 df 3f e5 70 71 88 dd 5e 07 d1 58 9b 9f 8b 66 30 55 3f 8f c3 52 b3 e0 c2 7d a8 0b dd ba 4c 64 02 0d	41 41 fd db 9c f2 45 86 d0 a2 ad 1f 11 1d a6 0e cf 26 40 6f f7 f1 e0 c6 e5 40 3a fb 4c d8 61 cb 33 e5 70 73 48 dd 5e 17 65 58 9b 83 a7 66 30 51 83 8f c3 4a 03 e0 c2 6d a8 0b dd b6 f4 64 02 1d

**Figure 13:** Chosen-prefix collision for SHA-1. The colors show the prefix, the birthday bits, and the near-collision blocks. Both messages lead to the same SHA-1 value: 8ac60ba76f1999a1ab70223f225aefdc78d4ddc0

